AD-A130 978 A NUMERICAL METHOD FOR COMPUTING THE TRANSONIC FAN DUCT FLOW OVER A CENTE..(U) BOEING CO RENTON WASH COMMERCIAL AIRPLANE GROUP F E EHLERS 1974 D6-41078 1/1

UNCLASSIFIED F/G 12/1 NL

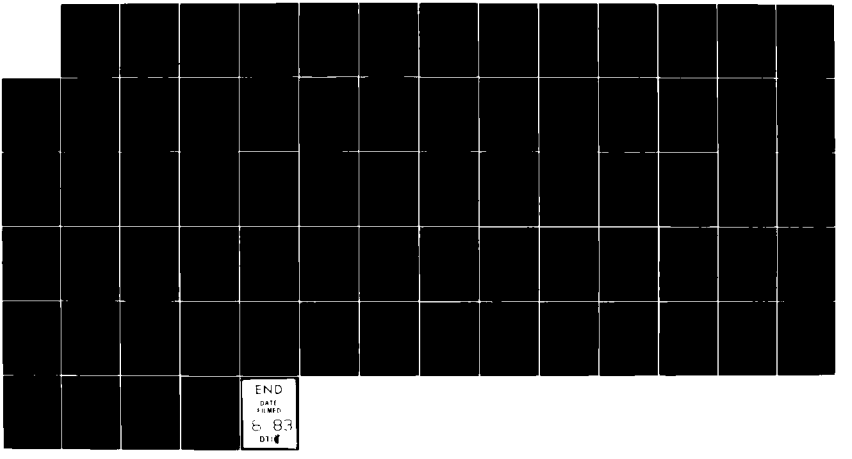

END
DATE FILMED
6 83
DTIC

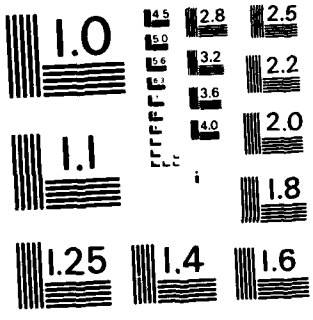

THE BOEING COMPANY

COMMERCIAL AIRPLANE DIVISION

RENTON, WASHINGTON

DOCUMENT NO. D6-41078

TITLE: A NUMERICAL METHOD FOR COMPUTING THE TRANSONIC FAN DUCT FLOW OVER A CENTERBODY INTO AN EXTERIOR FREE STREAM - PROGRAM TEA-343

MODEL

ISSUE NO. _____ TO: _____ (DATE)

PREPARED BY	F. E. Ehlers	3/14/73
SUPERVISED BY	P. E. Rubbert	9/24/74
APPROVED BY	B. Dillner	9/24/74
APPROVED BY		
		(DATE)

REV SYM

LIST OF ACTIVE PAGES

SECTION	PAGE NUMBER	REV SYM	ADDED PAGES					
			PAGE NUMBER	REV SYM	PAGE NUMBER	REV SYM	PAGE NUMBER	REV SYM
	1							
	2							
	3							
	4							
	5							
	6							
	7							
	8							
	9							
	10							
	11							
	12							
	13							
	14							
	15							
	16							
	17							
	18							
	19							
	20							
	21							
	22							
	23							
	24							
	25							
	26							
	27							
	28							
	29							
	30							
	31							
	32							
	33							
	34							
	35							
	36							
	37							
	38							
	39							
	40							
	41							
	42							
	43							
	44							
	45							
	46							
	47							
	48							
	49							
	50							

SECTION	PAGE NUMBER	REV SYM	ADDED PAGES					
			PAGE NUMBER	REV SYM	PAGE NUMBER	REV SYM	PAGE NUMBER	REV SYM
	51							
	52							
	53							
	54							
	55							
	56							
	57							
	58							
	59							
	60							
	61							
	62							
	63							
	64							
	65							
	66							
	67							
	68							
	69							
	70							
	71							
	72							

AD 15488

REV SYM

REVISIONS

REV SYM	DESCRIPTION	DATE	APPROVAL

Letter on file

A

AD 1546 C

REV SYM

J18-047

TABLE OF CONTENTS

D1 4100 7740 ORIG.8/71

TABLES

LIST OF FIGURES

1. Summary and Introduction

A theory and computer program are presented for computing the transonic fan duct and free jet flow exhausting over the centerbody of a turbofan engine and merging with an exterior stream flowing over a nacelle. The physical problem under consideration is sketched in Figure 1. For simplicity, the primary jet is treated as a solid circular body. The exterior stream and fan duct flows are both inviscid and are represented by appropriate differential equations based on nonlinear transonic small disturbance theory. The position of the free jet boundary is found as part of the solution by imposing the free slip boundary condition of continuity of pressure and slope at the linearized boundary interface. The Mach number of the expanded jet at downstream infinity where the static pressure is ambient is specified, and this, in turn, establishes the total pressure of the jet flow by means of the isentropic relation. The total jet mass flux is not a free parameter but is determined as a part of the solution by the choice of the downstream jet Mach number and application of the Kutta condition at the trailing edge of the fan cowl. The mass flux at the fan plane (see Fig. 1) is assumed to be uniformily distributed. Also required is the distribution of axial velocity along a transverse plane exterior to the nacelle and upstream of the fan exit (see Fig. 1), and the Mach number of the undisturbed external flow at infinity.

Numerical solutions are obtained by finite difference algorithms based on the original developments of Murman, Cole, and Krupp (Refs. 1-9). Figure 2b shows a typical example of computed streamline patterns, jet boundary slope and sonic lines. For this particular example, there

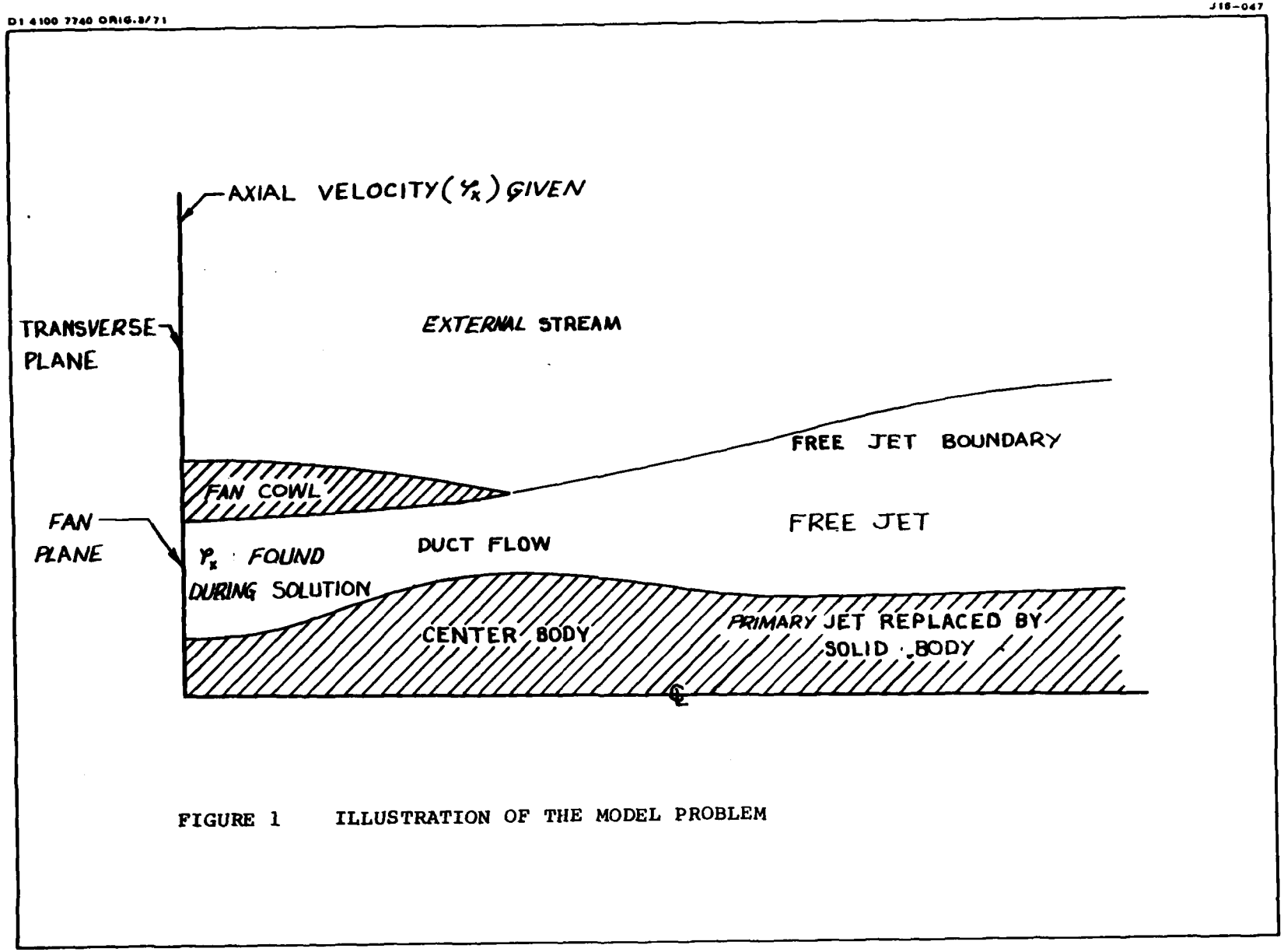

FIGURE 1 ILLUSTRATION OF THE MODEL PROBLEM

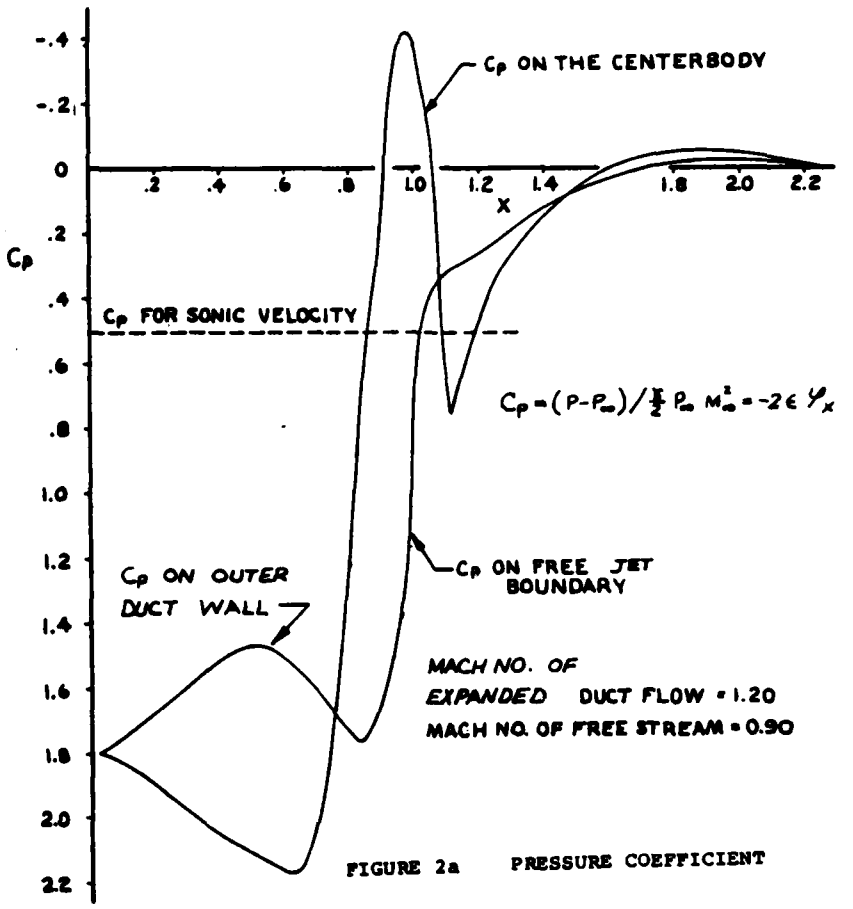

FIGURE 2a PRESSURE COEFFICIENT

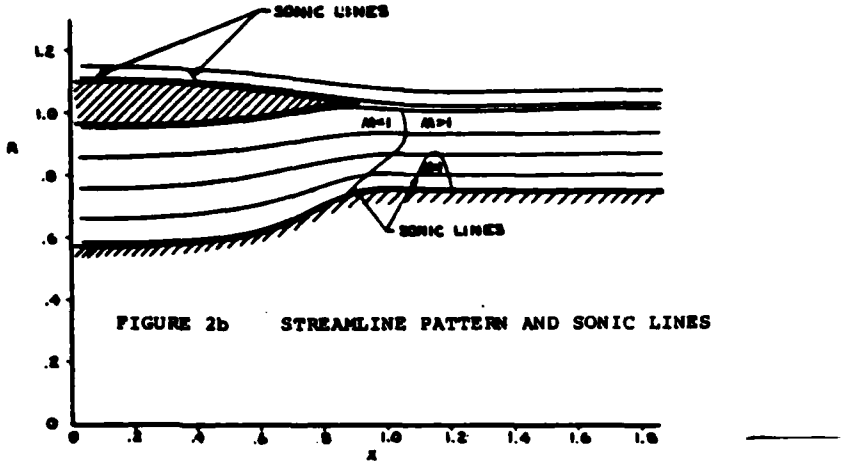

FIGURE 2b STREAMLINE PATTERN AND SONIC LINES

FIGURE 2 PRESSURE DISTRIBUTION, SONIC LINES, AND STREAMLINE PATTERN FOR EXAMPLE FLOW

occurred an imbedded region of subsonic flow adjoining the centerbody downstream of the fan cowl exit plane. Figure 2a shows the corresponding pressure distributions on the centerbody, on the interior wall of the fan duct and along the free streamline dividing the jet and the exterior flow. No comparisons have yet been made with experimental data.

This report presents a complete derivation of the theory, a description of the finite difference procedures employed, and several examples of calculated flows. A description of the computer program is given in the Appendices together with instructions for its use.

2. Derivation of the Transonic Small Perturbation Differential Equations for the Flow in the Duct and in the External Stream

Since the entropy change across a weak shock is third order in the pressure jump, we shall assume irrotational flow and introduce a velocity potential Φ which satisfies the following differential equation:

$$\Phi_{xx}(a^2-\Phi_x^2)+\Phi_{r_1 r_1}(a^2-\Phi_{r_1})-2\Phi_{xr_1}\Phi_x\Phi_{r_1}+a^2\Phi_{r_1}/r_1=0 \quad (1)$$

where x and r_1 are the dimensionless axial and radial coordinates based on duct length, and a is the local velocity of sound given by

$$a^2=a_\infty^2+(\gamma-1)(U_\infty^2-\Phi_x^2-\Phi_{r_1}^2)/2 \quad (2)$$

with U_∞ denoting the velocity at infinity downstream. We now introduce a perturbation velocity potential φ with a small parameter ϵ in the form:

$$\Phi=U_\infty(x+\epsilon\varphi)$$

Since small disturbances are propagated normal to the principal flow direction in a nearly sonic free stream, we introduce a scaling factor in the r_1 direction. This is expressed by

$$r=\tau r_1$$

where τ and ϵ will be determined appropriately in the following development.

Boundary conditions on the body are linearized. Let $r_b(x) = d/2 + \delta R_u(x)$ define the boundary of the nacelle adjoining the free stream. Here δ is a thickness ratio associated with either the nacelle or the centerbody. At $r_1 = d/2$, the boundary condition that the flow be tangential to the nacelle wall becomes

$$\phi_{r_1} / \phi_x = \delta R_u'(x)$$

Substituting the perturbation velocity potential yields

$$\tau \epsilon \varphi_r / (1 + \epsilon \varphi_x) \simeq \tau \epsilon \varphi_r = \delta R_u'(x) \tag{3}$$

It is convenient to let

$$\tau = \delta / \epsilon \tag{4}$$

and the boundary condition takes the familiar linearized form

$$\varphi_r = R_u'(x) \quad at \quad r = \tau r_1 = \tau d/2 \tag{5}$$

The velocity of sound to the first order in ϵ becomes

$$a^2/U_\infty^2 = 1/M_\infty^2 - (\gamma-1)\epsilon \varphi_x + O(\epsilon^2) \tag{6}$$

Substituting the preceding relation for a^2/U_∞^2 into the differential equation (1) and neglecting terms of the order of ϵ^2 yield

$$\varphi_{xx}\left[\frac{1-M_\infty^2}{\epsilon M_\infty^2} - (\gamma+1)\varphi_x\right] + \frac{\tau^2}{\epsilon M_\infty^2}\left[\varphi_{rr} + \varphi_r/r\right] = O(\epsilon) \tag{7}$$

We consider the limit as M_∞ approaches unity while the perturbation parameter ϵ approaches zero. Thus, we define the limit

$$(1-M_\infty^2)/\epsilon M_\infty^2 \to K$$

Letting

$$\tau^2 = \epsilon M_\infty^2 \tag{8}$$

renders the r derivatives of the same order as the x derivative and yields the well known transonic small perturbation differential equation in the form

$$[K - (\gamma+1)\varphi_x]\varphi_{xx} + (r\varphi_r)_r / r = 0 \tag{9}$$

Equations (8) and (4) enable us to determine ϵ and τ in terms of the free stream Mach number and thickness ratio δ ; i.e.,

$$\tau = M_\infty^{2/3} \delta^{1/3} \tag{10}$$

and

$$\epsilon = \delta^{2/3} / M_\infty^{2/3} \tag{11}$$

Also for K, we have

$$K = (1 - M_\infty^2) / \delta^{2/3} M_\infty^{4/3}$$

Note that in the limiting process we retained some non-linearity in the differential equation. Equation (9) is elliptic when

$$\varphi_x < K/(\gamma+1)$$

and hyperbolic when

$$\varphi_x > K/(\gamma+1)$$

The quantity $K/(\gamma+1)$ is the sonic velocity.

We now apply a similar approach to the duct flow. Let M_j be the Mach number at infinity downstream where the duct flow and outside stream have

the same static pressure. Then for the perturbation velocity potential we define

$$\Phi = U_j (x + \epsilon_j \varphi) \tag{12}$$

The velocity of sound in the duct is given by a relation similar to Eq. (6) i.e.,

$$a^2/U_j^2 = 1/M_j^2 - (\gamma-1)\epsilon_j \varphi_x + O(\epsilon_j^2) \tag{13}$$

Substituting Eqs. (12) and (13) into the differential equation (1) leads to the equation

$$\left[\frac{1-M_j^2}{\epsilon_j M_j^2} - (\gamma+1)\varphi_x\right]\varphi_{xx} + \frac{\tau^2}{\epsilon_j M_j^2}(\varphi_{rr} + \varphi_r/r) = O(\epsilon_j) \tag{14}$$

We shall retain the same scaling factor τ as in the outside stream. Thus

$$\tau^2 = \epsilon_j M_j^2 = \epsilon M_\infty^2 \tag{15}$$

and

$$\epsilon_j = \epsilon M_\infty^2 / M_j^2 \tag{16}$$

The transonic parameter K_1 for the duct flow is

$$K_1 = (1-M_j^2)/\epsilon_j M_j^2 = (1-M_j^2) K/(1-M_\infty^2) \tag{17}$$

and the differential equation for flow inside the duct becomes

$$[(1-M_j^2)K/(1-M_\infty^2) - (\gamma+1)\varphi_x]\varphi_{xx} + (r\varphi_r)_r/r = 0 \tag{18}$$

For the duct walls defined by $r_1 = d/2 + \delta R_L(x)$, the linearized boundary

conditions take the form

$$\bar{\phi}_{r_1} / \bar{\phi}_x \simeq \epsilon_j \tau \varphi_r = \delta R_L'(x) \tag{19}$$

or

$$\varphi_r = M_j^2 R_L'(x) / M_\infty^2 \tag{20}$$

The transonic small perturbation differential Eqs. (9) and (18) are non-linear and practical analytical solutions are difficult to obtain. In the sequel, the equations are expressed in difference form and numerical relaxation techniques are applied to find the solutions for specific flow configurations.

3. The Pressure Coefficient for the Transonic Small Perturbation Theory

We shall now find the relation for the pressure coefficient as calculated from the solution of φ from the transonic small perturbation differential equation. From Bernouilli's relation, Eq. (2), and the definition of φ , we have

$$a^2/a_\infty^2 = 1 + \frac{(\gamma-1)}{2}\left[1 - (1+\epsilon\varphi_x)^2 + O(\epsilon^2)\right]$$
$$= 1 - (\gamma-1)M_\infty^2 \epsilon \varphi_x + O(\epsilon^2)$$

For the pressure p in terms of a, we have

$$p/p_\infty = (a^2/a_\infty^2)^{\gamma/(\gamma-1)} = 1 - \gamma M_\infty^2 \epsilon \varphi_x + O(\epsilon^2)$$

Introducing the pressure coefficient yields.

$$C_{p_\infty} = (p - p_\infty)/\tfrac{1}{2} p_\infty M_\infty^2 = -2\epsilon\varphi_x$$

Following a similar procedure for the duct flow we obtain for the pressure coefficient,

$$C_{p_j} = (p - p_j) \Big/ \frac{\gamma p_j M^2}{2} = -2\epsilon_j \varphi_x = -2\epsilon M_\infty^2 \varphi_x / M_j^2$$

Since the pressures of the two streams balance at infinity, $P_j = P$ and the condition that the pressure balance on the boundary streamline between the two flows is easily seen to be

$$\varphi_x^{(\infty)} = \varphi_x^{(j)}$$

where the superscripts ∞ and j denote the limits of freestream and duct velocity perturbation potentials, respectively, as one approaches the boundary streamline.

4. Rate of Mass Flow in the Stream Direction

The magnitudes of φ_x at the fan plane evolves as a part of the solution and is subject to periodic updating during the course of the relaxation procedure. For this purpose, we derive a formula for the mass flow rate which is required for updating φ_x as the computation progresses. Neglecting the cross component of velocity, we obtain the following relation for the local density in the jet

$$\rho/\rho_j = (a^2/a_j^2)^{1/(\gamma-1)} = [1 - (\gamma-1)M_j^2(\epsilon_j \varphi_x + \epsilon_j^2 \varphi_x^2/2 \cdots)]^{\frac{1}{\gamma-1}}$$

Expanding and retaining terms to the order of ϵ_j^2 yields

$$\rho/\rho_j = 1 - M_j^2[\epsilon_j \varphi_x + \epsilon_j^2 \varphi_x^2/2] + \frac{2-\gamma}{2} M_j^4 \epsilon_j^2 \varphi_x^2 + O(\epsilon_j^3) \qquad (21)$$

This may be written in the following form by regrouping the second order terms:

$$\rho/\rho_j = 1 - M_j^2 \epsilon_j \varphi_x - (\gamma-1) M_j^4 \epsilon_j^2 \varphi_x^2/2 + \epsilon_j^2 M_j^2 (M_j^2-1) \varphi_x^2/2 \qquad (22)$$

Since $M_j^2 \epsilon_j^2 (M_j^2-1) = -\epsilon_j^3 M_j^4 K = O(\epsilon^3)$ the third term may be neglected.

The rate of mass flow per unit area then is given by

$$\rho \underline{\Phi}_x \Big/ \rho_j U_j = [1 - M_j^2 \epsilon_j \varphi_x - (\gamma-1) M_j^4 \epsilon_j^2 \varphi_x^2/2][1 + \epsilon_j \varphi_x] + O(\epsilon^3) \qquad (23)$$

We note that this may be written

$$\rho \underline{\Phi}_x \Big/ \rho_j U_j = 1 + \epsilon_j (1-M_j^2) \varphi_x - (\gamma+1) M_j^4 \epsilon_j^2 \varphi_x^2/2 + M_j^2 (M_j^2-1) \epsilon_j^2 \varphi_x^2 \qquad (24)$$

The last term is seen to be of higher order than the preceding terms. The reason for retaining second order terms in ϵ^2 becomes apparent when we introduce

$$\epsilon_j (1-M_j^2) = \epsilon_j^2 M_j^2 K_1 \simeq \epsilon_j^2 K_1$$

and

$$M_j^2 \simeq 1 + O(\epsilon_j)$$

into Eq. (24) and obtain

$$\rho \underline{\Phi}_x / \rho_j U_j = 1 + \epsilon_j^2 [K_1 \varphi_x - (\gamma+1) \varphi_x^2/2] \qquad (25)$$

Note that the mass flow is a maximum when the flow is sonic, i.e., at

$$\varphi_x = K_1/(\gamma+1) \qquad (26)$$

Solving Equation (25) for φ_x yields

$$\varphi_x = [K_1 - \sqrt{K_1^2 - 2(\gamma+1) m/\epsilon_j^2}\,]/(\gamma+1) \qquad (27)$$

where $m = (\rho \underline{\Phi}_x - \rho_j U_j)/\rho_j U_j$.

With the mass flow rate m computed from an intermediate solution, the value for φ_x at the fan plane is updated in terms of the values of φ_x from Equation (27), keeping the total mass flux in the jet fixed. A relation similar to Eq. (27) for the exterior stream is easily written down by replacing K_1 and ϵ_j by K and ϵ, respectively.

5. The Physical Problem to be Solved and the Development of the Boundary Value Problem

We are interested in finding the pressure distribution over the back part of a nacelle and on the duct centerbody over which the air from the fan flows. The problem is idealized to the flow field illustrated in Figure 1 with a solid body replacing the central jet flow. Since we linearize the boundary conditions on the solid boundaries and on the free streamline boundary between the duct flow and the outside stream, the idealized flow is expressed as a boundary value problem for the perturbation velocity potential. This is presented in Figure 3.

The boundary value problem appears to be well posed, since the value of the potential or its normal derivative is prescribed on the boundary. However, the application of a Kutta condition at the fan cowl trailing edge is an additional restriction which requires that the magnitude of φ_x at the fan plane not be arbitrary, but must be determined from the solution of the problem. This value is found from computing the mass flow in the free jet far downstream and determining the value of $\varphi_{\bar{x}}$ at the fan plane which satisfies conservation of mass in the duct and jet. The mass flow from the duct calculated far downstream is not a sensitive function of the initial guess for $\varphi_{\bar{x}}$ at the fan plane (which must be input) but is dependent ultimately upon the choice of undisturbed free jet Mach number because of the Kutta condition. The input fan

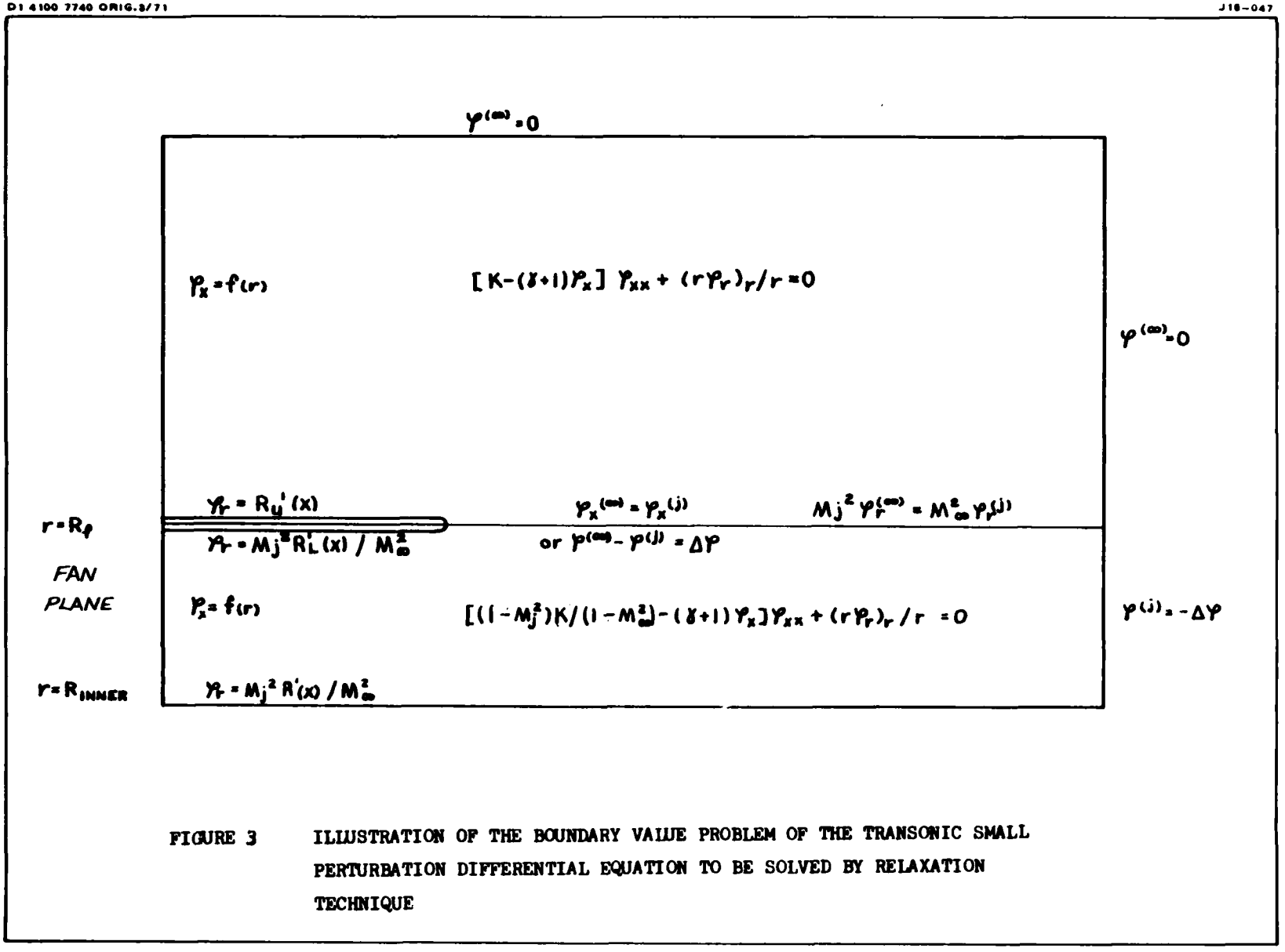

FIGURE 3 ILLUSTRATION OF THE BOUNDARY VALUE PROBLEM OF THE TRANSONIC SMALL PERTURBATION DIFFERENTIAL EQUATION TO BE SOLVED BY RELAXATION TECHNIQUE

plane boundary conditions are corrected from calculations of the conservation of mass as the solution progresses. The freestream Mach number M_∞ and the free jet Mach number, M_j, are two parameters which must be fixed in the calculations.

The differential equations in the two regions are expressed in difference form and the flow field computed by means of relaxation techniques.

6. The Difference Equation for the Interior Points of the Flow

To apply relaxation techniques to the boundary value problem in Fig. 3, we divide the region into a rectangular mesh by lines parallel to the x and r axes. The spacing is generally not uniform as greater accuracy is achieved in minimum computing time by using a finer spacing near boundaries for the r variable and finer spacing near rapidly accelerating or decelerating regions of the flow in the x variable. Let the subscripts i, j denote the values of the variables at typical interior points given by the coordinates x_i, r_j. The second derivative in the x direction at $x = x_i$ and $r = r_j$ is expressed in difference form for subsonic flow by using the values at points on the both sides of the point i,j and is easily seen to be

$$\varphi_{xx} = \left[\frac{\varphi_{i+1\,j} - \varphi_{i\,j}}{x_{i+1} - x_i} - \frac{\varphi_{i\,j} - \varphi_{i-1\,j}}{x_i - x_{i-1}} \right] \frac{2}{(x_{i+1} - x_{i-1})}$$

$$= 2c_i \varphi_{i+1\,j} - 2e_i \varphi_{i\,j} + 2d_i \varphi_{i-1\,j} \qquad (28)$$

where

$$c_i = 1/(x_{i+1} - x_{i-1})(x_{i+1} - x_i)$$
$$d_i = 1/(x_i - x_{i-1})(x_{i+1} - x_{i-1}) \qquad (29)$$
$$e_i = 1/(x_i - x_{i-1})(x_{i+1} - x_i)$$

The notation as used here is suggestive of the notation used in the Fortran statements of the computer programs in order to make it easy for the user to understand the computer programs from this discussion.

For the derivative with respect to r, we use a similar central difference formula, for both subsonic and supersonic flow.

$$(r\varphi_r)_r/r = \left\{ r_{j+1/2}\frac{(\varphi_{i,j+1}-\varphi_{i,j})}{r_{j+1}-r_j} - r_{j-1/2}\frac{(\varphi_{i,j}-\varphi_{i,j-1})}{(r_j-r_{j-1})} \right\} \frac{2}{r_j(r_{j+1}-r_{j-1})}$$

$$= 2a_j\varphi_{i,j-1} - 2(a_j+b_j)\varphi_{i,j} + 2b_j\varphi_{i,j-1} \qquad (30)$$

where

$$a_j = r_{j-1/2}/r_j(r_{j+1}-r_{j-1})(r_j-r_{j-1})$$
$$b_j = r_{j+1/2}/r_j(r_{j+1}-r_{j-1})(r_{j+1}-r_j) \qquad (31)$$

and we introduce the convenient notation

$$r_{j\pm1/2} = (r_j + r_{j\pm1})/2 \qquad (32)$$

To complete the difference form of the differential equation, we require a representation of the first derivative with respect to x. For points equally spaced a Δx apart, the difference form

$$(\varphi_{i+1,j} - \varphi_{i-1,j})/2\Delta x$$

approximates φ_x to the second order in Δx at the central point i,j. To obtain a second order form for φ_x when the points are not equally spaced, we write

$$\varphi_x = c_{1i}(\varphi_{i+1,j} - \varphi_{ij}) + d_{1i}(\varphi_{ij} - \varphi_{i-1,j}) \tag{33}$$

and determine c_{1i} and d_{1i} appropriately by Taylors series expansions about ij. Let $h_1 = x_{i+1} - x_i$ and $h_2 = x_i - x_{i-1}$. Then expanding about the point i,j yields

$$\begin{aligned} &c_{1i}(h_1\varphi_x + h_1^2\varphi_{xx}/2 + h_1^3\varphi_{xxx}/6 + \cdots) \\ &+ d_{1i}(h_2\varphi_x - h_2^2\varphi_{xx}/2 + h_2^3\varphi_{xxx}/6 + \cdots) = \varphi_x \end{aligned} \tag{34}$$

Setting the coefficient of φ_x equal to 1 and the coefficient of the φ_{xx} term equal to zero yields two linear equations to solve for c_{1i} and d_{1i}. The result is

$$c_{1i} = h_2/h_1(h_1+h_2) = \frac{x_i - x_{i-1}}{(x_{i+1} - x_{i-1})(x_{i+1} - x_{i-1})} = (x_i - x_{i-1})c_i$$

$$d_{1i} = (x_{i+1} - x_i)d_i \tag{35}$$

For inside the duct we define the difference form

$$\begin{aligned} v_{ij} &= (1-M_j^2)\pi/(1-M_\infty^2) - (\gamma+1)\varphi_x \\ &= (1-M_j^2)\pi/(1-M_\infty^2) - (\gamma+1)[c_{1i}(\varphi_{i+1,j} - \varphi_{ij}) \\ &\quad + d_{1i}(\varphi_{ij} - \varphi_{i-1,j})] \end{aligned} \tag{36}$$

and for the outside stream, we use

$$u_{ij} = \pi - (\gamma+1)[c_{1i}(\varphi_{i+1,j} - \varphi_{ij}) + d_{1i}(\varphi_{ij} - \varphi_{i-1,j})] \tag{37}$$

By applying Eqs. (28), (30), and (36) to the differential equation (18) when the flow in the duct is subsonic, we obtain the following difference equation

$$2v_{ij}(c_i\varphi_{i+1,j} - e_i\varphi_{ij} + d_i\varphi_{i-1,j}) + 2[a_j\varphi_{i,j-1} - (a_j+b_j)\varphi_{ij} + b_j\varphi_{i,j+1}] = 0 \tag{38}$$

In the relaxation process, we solve for the values of φ along a column $x = x_i$ in the flow. It is therefore more convenient to write Eq. (38) as

$$a_j\varphi_{i,j-1} - (v_{ij}e_i + a_j + b_j)\varphi_{ij} + b_j\varphi_{i,j+1} = -v_{ij}(c_i\varphi_{i+1,j} + d_i\varphi_{i-1,j}) \tag{39}$$

In this form, with v_{ij} regarded as fixed, a set of linear equations for the values of φ along $x = x_i$ results. The matrix of coefficients is tri-diagonal and is easy to solve. The non-linear equation is solved by iteration. The quantity v_{ij} is defined by the values of φ from the previously iteration and then φ is found from solving Eq. (39). The calculations are repeated with v_{ij} determined by the recently obtained values of φ. The iteration is continued until the required accuracy is achieved.

When the flow is supersonic, i.e., when $v_{ij} < 0$, we use a backward difference formula in the axial variable x instead of the central difference formula described above.

Hence,

$$[\kappa_1 - (\gamma+1)\varphi_x]\varphi_{xx}\Big|_{x_i} = v_{i-1,j}(c_{i-1}\varphi_{ij} - e_{i-1}\varphi_{i-1,j} + d_{i-1}\varphi_{i-2,j}) \tag{40}$$

With Eq. (40) substituted for the first term in Eq. (38), we obtain the following equation equivalent to Eq. (39) for supersonic flow:

$$a_j \varphi_{i,j-1} + (V_{i-1,j} c_{i-1} - a_j - b_j) \varphi_{ij} + b_j \varphi_{i,j+1} = + V_{i-1,j} (e_{i-1} \varphi_{i-1,j} - d_{i-1} \varphi_{i-2,j}) \quad (41)$$

The points at which $v_{ij} < 0$ but $v_{i-1j} > 0$ are parabolic. When this occurs, Eq. (41) is modified by setting $v_{i-1\ j} = 0$.

For the interior points of the outside stream, similar equations result but with $u_{i,j}$ and $u_{i-1,j}$ replacing $v_{i,j}$ and $v_{i-1,j}$, respectively.

7. The Application of Wall Boundary Conditions to the Difference Equation at Mesh Points Adjacent to Boundaries

The application of the boundary conditions near a solid wall is more easily made when the mesh points are not included on the boundary but a half mesh point width away. Consider first the lower boundary. Figure 4 shows the points i, j = 1 and 2 and the boundary point where the boundary condition is applied. The r derivative becomes

$$\frac{1}{r}(r\varphi_r)_r = \frac{2}{r_1(r_0 - r_2)} \left\{ r_b \varphi_r - r_{3/2} \frac{(\varphi_{i1} - \varphi_{i2})}{r_1 - r_2} \right\} \quad (42)$$

where for convenience we choose $r_0 = r_b - (r_1 - r_b) = 2r_b - r_1$. From Fig. 3, the introduction of the boundary condition yields

(43)

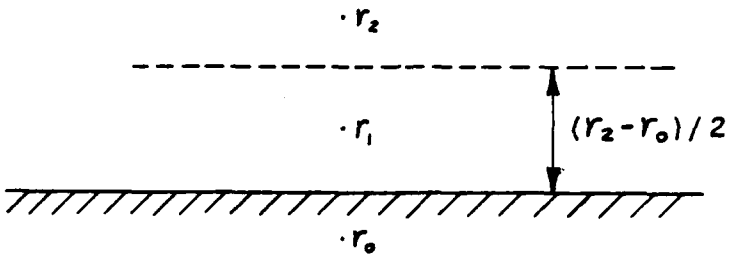

FIGURE 4 COLUMN MESH POINTS ILLUSTRATING THE APPLICATION OF THE LOWER BOUNDARY CONDITION

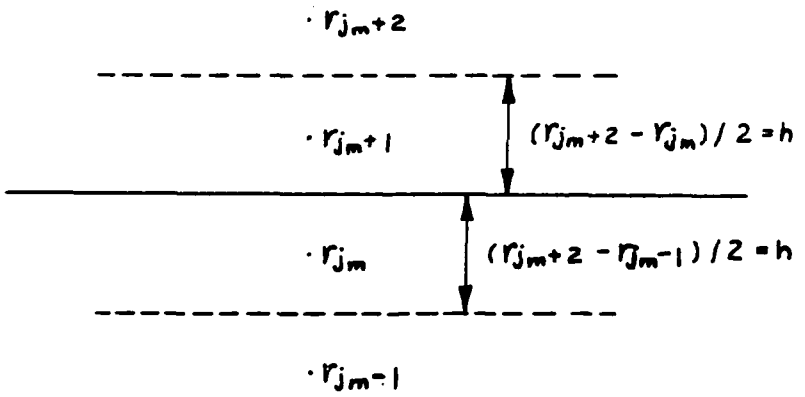

FIGURE 5 COLUMN MESH POINTS ILLUSTRATING THE APPLICATION OF THE UPPER BOUNDARY CONDITIONS AND THE CONTINUITY ACROSS THE FREE STREAMLINE

AD 1346D

$$\frac{1}{r}(r\varphi_r)_r = -\frac{2r_b M_j^2 R'(x_i)}{r_1(r_2-r_0)M_\infty^2} + 2b_1(\varphi_{i2}-\varphi_{i1})$$

$$= 2b_1(\varphi_{i2}-\varphi_{i1}) - 2\alpha_1 R_i'$$

where

$$\alpha_1 = r_b M_j^2 / r_1 M_\infty^2 (r_2 - r_0)$$

The difference form of the differential equation then becomes

$$V_{ij}(c_i\varphi_{i+1,1} - e_i\varphi_{i1} + d_i\varphi_{i-1,1}) + b_1(\varphi_{i2}-\varphi_{i1}) - \alpha_1 R_i' = 0 \tag{44}$$

Rewriting in tridiagonal form for the ith column relaxation yields

$$-(b_1 + e_i V_{i1})\varphi_{i1} + b_1\varphi_{i2} = -V_{i1}(c_i\varphi_{i+1,1} + d_i\varphi_{i-1,1}) + \alpha_1 R_i' \tag{45}$$

When the point is supersonic, we have instead,

$$(V_{i-1,1}e_{i-1} - b_1)\varphi_{i1} + b_1\varphi_{i2} = V_{i-1,1}(c_{i-1}\varphi_{i-1,1} - d_{i-1}\varphi_{i-2,1}) + \alpha_1 R_i' \tag{46}$$

For the upper boundary, situated at $r = r_f$, halfway between the r_{j_m} and r_{j_m+1}, we obtain a similar relation of the r derivative (see Fig. 5).

$$\frac{1}{r}(r\varphi_r)_r = \frac{2}{r_{j_m}(r_{j_m-1}-r_{j_m+1})}\left\{\frac{r_{j_m-1/2}(\varphi_{ij_m}-\varphi_{ij_{m-1}})}{r_{j_m}-r_{j_{m-1}}} - r_f\varphi_r\right\} \tag{47}$$

$$= -2a_{j_m}(\varphi_{ij_m}-\varphi_{ij_{m-1}}) + 2\alpha_2 R_L'(x_i)$$

where $\alpha_2 = M_j^2 r_f / r_{j_m}(r_{j_m+1} - r_{j_m-1}) M_\infty^2$. (48)

The equation equivalent to Eq. (45) then becomes

$$a_{j_m} \varphi_{i j_m-1} - (v_{i j_m} e_i + a_{j_m}) \varphi_{i j_m} = -v_{ij}(c_i \varphi_{i+1, j_m} + d_i \varphi_{i-1 j_m}) - \alpha_2 R'_{\perp i} \quad (49)$$

When $v_{ij_m} < 0$, then Eq. (49) becomes

$$a_{j_m} \varphi_{i j_m-1} + (v_{i-1 j_m} c_{i-1} - a_{j_m}) \varphi_{i j_m} = v_{i-1 j_m}(e_{i-1} \varphi_{i-1 j_m} - d_{i-1} \varphi_{i-2 j_m}) - \alpha_2 R'_{\perp i} \quad (50)$$

For the point $r = r_{j_m} + 1$, the application of the boundary condition in Fig. 2 by comparison with Eq. (45) is seen to yield

$$-(u_{i j_m+1} e_i + b_{j_m+1}) \varphi_{i j_m+1} + b_{j_m+1} \varphi_{i j_m+2} = -u_{i j_m+1}(c_i \varphi_{i+1, j_m+1} + d_i \varphi_{i-1 j_m+1}) + \alpha_3 R'_{u i} \quad (51)$$

where $\alpha_3 = r_f / r_{j_m+1}(r_{j_m+2} - r_{j_m})$. (52)

A formula for the hyperbolic case analogous to Eq. (46) for the outside stream may easily be written down.

8. Application of the Prescribed Inlet Flow Condition to the Difference Equation

Along the line x = 0 in the duct as well as in the outside stream, we prescribe the values of φ_x at the points of the mesh $r = r_j$, j = 1 to j_{max}. Let $\varphi_x = f(r)$ at x = 0 and define $f_j = f(r_j)$. For φ_x at $x = x_1$, we follow a procedure similar to that used for the r boundary conditions.

For convenience we introduce the potential

$$\psi = \kappa x - (\gamma+1)\varphi$$

Then the x derivative term of the differential equation becomes

$$[\kappa - (\gamma+1)\varphi_x]\varphi_{xx} = -\psi_x \psi_{xx}/(\gamma+1) = -(\psi_x)_x^2/2(\gamma+1) \tag{53}$$

Expressing this quantity in difference form leads to

$$(\psi_x^2)_x = 2\left[(\psi_x^{(3/2)})^2 - (\psi_x^{(0)})^2\right]/(x_2 - x_0) \tag{54}$$

where the superscripts 3/2 and 0 denote the value of ψ_x at $x = (x_1 + x_2)/2$ and $x = 0$, respectively. We define $x_0 = -x_1$, and we obtain, after factoring Eq. (54),

$$(\psi_x^2)_x = 2\left[\psi_x^{(3/2)} + \psi_x^{(0)}\right]\left[\psi_x^{(3/2)} - \psi_x^{(0)}\right]/(x_2 + x_1)$$

Since $\varphi_x = f_j$, we have $\psi_x^{(0)} = \kappa - (\gamma+1) f_j$ and

$$(\psi_x^2)_x = \frac{2}{x_2+x_1}\left[\frac{\psi_2 - \psi_1}{x_2 - x_1} - \kappa + (\gamma+1)f_j\right]\left[\frac{\psi_2 - \psi_1}{x_2 - x_1} + \kappa - (\gamma+1)f_j\right] \tag{55}$$

Replacing the variable φ yields

$$(\psi_x^2)_x = -\frac{2(\gamma+1)}{x_2+x_1}\left[\frac{\varphi_{2j} - \varphi_{1j}}{x_2 - x_1} - f_j\right]\left[2\kappa - (\gamma+1)\left(\frac{\varphi_{2j} - \varphi_{1j}}{x_2 - x_1} + f_j\right)\right] \tag{56}$$

We define $u_{ij} = \kappa - \frac{\gamma+1}{2}\left[\frac{\varphi_{2j}-\varphi_{1j}}{x_2-x_1} + f_j\right]$. (57)

To make the notation consistent with the nomenclature for general values of x, we write

$$u_{ij} = \kappa - (\gamma+1)\left[c_{11}(\varphi_{2j}-\varphi_{1j}) + d_{11} f_j\right] \tag{58}$$

where $c_{11} = 1/2(x_2 - x_1)$ and $d_{11} = 1/2$. The differential equation at the point $x = x_1$ and $r = r_j$ takes the following difference form

$$u_{ij}\left[\frac{\varphi_{2j}-\varphi_{1j}}{x_2^2 - x_1^2} - \frac{f_j}{x_2+x_1}\right] + a_j \varphi_{2,j-1} - (a_j+b_j)\varphi_{1j} + b_j \varphi_{1,j+1} = 0 \tag{59}$$

Expressed in tridiagonal form, this becomes

$$a_j \varphi_{1,j-1} - (a_j + b_j + c_1 u_{ij})\varphi_{1j} + b_j \varphi_{1,j+1} = u_{1j}(d_1 f_j - c_1 \varphi_{2j}) \tag{60}$$

where $c_1 = 1/(x^2_2 - x^2_1)$ and $d_1 = 1/(x_2 + x_1)$. Similar equations may readily be written for the duct equation with v_{ij} defined by Eq. (56) with k replaced by $(1 - M_j^2)k/(1 - M_\infty^2)$. The relation for $j = 1$ and $j = j_m + 1$ is easily found by setting $a_1 = 0$ and adding the appropriate boundary term to the right hand side. Similarly for $j = j_m$, b_{jm} is set equal to zero and the term $-a_{j_m} R'_{2j}$ added to the right hand side.

For subsonic points in the flow field, over-relaxation is employed by the program in the manner of Murman (8). However, it was found that over-relaxation at the inlet interfered with the satisfaction of the φ_x boundary condition at x = 0. This was remedied by varying the relaxation parameter w continuously from unity at x = 0 to about 1.3 to 1.7 at x = X(10).

9. Application of the Boundary Conditions for the Interface Between the Free Stream and the Duct Flow

The boundary conditions of continuity of slope and pressure across the free streamline boundary will be applied at the line

$$r = r_f = (r_{j_m} + r_{j_{m+1}})/2 \tag{61}$$

for $x > x_{i_0}$ or $i > i_0$. We have shown that the relations between the streamline slope and the r derivative for both the interior and exterior flows are

$$\varphi_r^{(j)} = M_j^2 R_s' / M_\infty^2$$
$$\varphi_r^{(\infty)} = R_s'$$

Continuity of slope across the streamline then yields

$$M_\infty^2 \varphi_r^{(j)} = M_j^2 \varphi_r^{(\infty)} \tag{62}$$

For the continuity of pressure we have

$$\varphi_x^{(j)} = \varphi_x^{(\infty)}$$

Since this relation must hold at all points of the free streamline, we can integrate from the trailing edge point to the point x_i. We obtain

$$\varphi^{(\infty)}(x_{i_0}) - \varphi^{(j)}(x_{i_0}) = \varphi^{(\infty)}(x) - \varphi^{(j)}(x)$$

Letting $\Delta\varphi = \varphi_{i_0}^{(\infty)} - \varphi_{i_0}^{(j)}$ we restate our boundary condition as

$$\varphi^{(\infty)}(x_i, r_f) - \varphi^{(j)}(x_i, r_f) = \Delta\varphi \tag{63}$$

The quantity $\Delta\varphi$ is a constant for the entire free streamline and is computed from the values at the trailing edge at each iteration.

We shall satisfy the boundary conditions on the free streamline at the centerline point between $r = r_{j_m}$ and $r = r_{j_m+1}$. To simplify the relations we shall further assume that the lines $r = r_{jm-1}$ to $r = r_{jm+2}$ are equally spaced a distance h. Since φ is defined only at the mesh points we apply Taylor's expansions to find φ at the midpoint $r = r_f = r_{jm+1/2}$. Thus, for φ on both sides of the free streamline, we have

$$\varphi^{(\infty)} = \varphi_{i,j_m+1} - \frac{h}{2}\varphi_r\Big|_{r=r_{j_m+1}} + \frac{h^2}{8}\varphi_{rr}\Big|_{r=r_{j_m+1}}$$

$$\varphi^{(j)} = \varphi_{i,j_m} + \frac{h}{2}\varphi_r\Big|_{r=r_{j_m}} + \frac{h^2}{8}\varphi_{rr}\Big)_{r=r_{j_m}} \qquad (64)$$

where we have dropped the superscripts on the right hand side since the subscript adequately defines the φ values. In the preceding two equations we replace φ_r and φ_{rr} derivatives by differences. As in Eqs. (33) through (35) for the x derivative, we develop a second order difference for φ and obtain

$$\varphi_r\Big|_{r=r_{j_m+1}} = (\varphi_{i,j_m+2} + 3\varphi_{i,j_m+1} - 4\varphi^{(\infty)})/3h$$

$$\varphi_r\Big|_{r=r_{j_m}} = (4\varphi^{(j)} - 3\varphi_{i,j_m} - \varphi_{i,j_m-1})/3h \qquad (65)$$

Similarly for the second derivatives, we obtain

$$\varphi_{rr}\Big|_{r_{j_m+1}} = \left[\frac{\varphi_{i,j_m+2} - \varphi_{i,j_m+1}}{r_{j_m+2} - r_{j_m+1}} - \varphi_r^{(\infty)}\right]\frac{2}{(r_{j_m+2} - r_{j_m})}$$

$$= (\varphi_{i,j_m+2} - \varphi_{i,j_m+1})/h^2 - \varphi_r^{(\infty)}/h$$

$$\varphi_{rr}\Big|_{r_{j_m}} = \varphi_r^{(j)}/h - (\varphi_{i,j_m} - \varphi_{i,j_m-1})/h^2 \qquad (66)$$

Substitution of Eqs. (65) and (66) into Eqs. (64) and solving for $\varphi^{(\infty)}$ and $\varphi^{(j)}$ yields the following two equations for the values of φ on the two sides of the streamline

$$\varphi^{(\infty)} = -\varphi_{i,j_m+2}/8 + 9\varphi_{i,j_m+1}/8 - 3h\varphi_r^{(\infty)}/8$$
$$\varphi^{(j)} = 9\varphi_{i,j_m}/8 - \varphi_{i,j_m-1}/8 + 3h\varphi_r^{(j)}/8 \qquad (67)$$

Two more equations for $\varphi_r^{(\infty)}$ and $\varphi_r^{(j)}$ can be obtained from the difference forms of the partial differential equations at the mesh points i,j_m and i,j_m+1. The r derivative for $r = r_{j_m}$ takes a form similar to Eqs. (42) and (47); i.e.,

$$\frac{1}{r}(r\varphi_r)_r\Big|_{r=r_{j_m}} = \frac{1}{r_{j_m}}\left[r_{j_m}\varphi_r^{(j)} - \frac{r_{j_m-1/2}(\varphi_{i,j_m} - \varphi_{i,j_m-1})}{r_{j_m} - r_{j_m-1}}\right]\frac{2}{(r_{j_m+1} - r_{j_m-1})} \qquad (68)$$

From the definition of a_{j_m} and b_{j_m} we recognize that Eq. (68) may be written

$$\frac{1}{r}(r\varphi_r)_r\Big|_{r=r_{j_m}} = 2\left[hb_{j_m}\varphi_r^{(j)} - a_{j_m}(\varphi_{i,j_m} - \varphi_{i,j_m-1})\right] \qquad (69)$$

Similarly for $r = r_{j_m+1}$, we find that

$$\frac{1}{r}(r\varphi_r)_r\Big|_{r=r_{j_m+1}} = 2\left[b_{j_m+1}(\varphi_{i,j_m+2} - \varphi_{i,j_m+1}) - ha_{j_m+1}\varphi_r^{(\infty)}\right] \qquad (70)$$

Substituting Eqs. (69) and (70) into the difference form of the differential equations yields, for v_{ij_m} and $u_{ij_m+1} > 0$,

$$v_{ij_m}(c_i\varphi_{i+1j_m} - e_i\varphi_{ij_m} + d_i\varphi_{i-1j_m}) + hb_{j_m}\varphi_r^{(j)} - a_{j_m}(\varphi_{ij_m} - \varphi_{ij_{m-1}}) = 0 \tag{71}$$

$$u_{ij_{m+1}}(c_i\varphi_{i+1j_{m+1}} - e_i\varphi_{ij_{m+1}} + d_i\varphi_{i-1j_{m+1}}) - ha_{j_{m+1}}\varphi_r^{(\infty)} + b_{j_{m+1}}(\varphi_{ij_{m+2}} - \varphi_{ij_{m+1}}) = 0$$

For later convenience, we solve Eqs. (71) for φ_r^{∞} and $\varphi_r^{(j)}$ and rearrange the terms to obtain

$$\begin{aligned} hb_{j_m}\varphi_r^{(j)} &= -a_{j_m}\varphi_{ij_{m-1}} + A_2\varphi_{ij_m} + B_2 \\ ha_{j_{m+1}}\varphi_r^{(\infty)} &= b_{j_{m+1}}\varphi_{ij_{m+2}} + A_1\varphi_{ij_{m+1}} + B_1 \end{aligned} \tag{72}$$

where

$$\begin{aligned} A_1 &= -(e_i u_{ij_{m+1}} + b_{j_{m+1}}) \\ B_1 &= u_{ij_{m+1}}(c_i\varphi_{i+1j_{m+1}} + d_i\varphi_{i-1j_{m+1}}) \\ A_2 &= v_{ij_m}e_i + a_{j_m} \\ B_2 &= -v_{ij_m}(c_i\varphi_{i+1j_m} + d_i\varphi_{i-1j_m}) \end{aligned} \tag{73}$$

When the flow on either side is supersonic $(u_{ij} \text{ or } v_{ij} < 0)$, then Eq. (72) holds but with A_1, B_1, and A_2 and B_2 defined by

$$\begin{aligned} A_1 &= c_{i-1}u_{i-1j_{m+1}} - b_{j_{m+1}} \\ B_1 &= -u_{i-1j_{m+1}}[e_{i-1}\varphi_{i-1j_{m+1}} - d_{i-1}\varphi_{i-2j_{m+1}}] \\ A_2 &= a_{j_m} - c_{i-1}v_{i-1j_m} \\ B_2 &= v_{i-1j_m}(e_{i-1}\varphi_{i-1j_m} - d_{i-1}\varphi_{i-2j_m}) \end{aligned} \tag{74}$$

With the boundary conditions of Eqs. (62) and (63), the quantities $\varphi_r^{(j)}, \varphi_r^{(\infty)}, \varphi_j^{j}$ and $\varphi^{(\infty)}$ may be eliminated from Eqs. (67) and (72). Using Eqs. (62) in the form

$$a_{j_m+1} M_\infty^2 (h b_{j_m} \varphi_r^{(3)}) - b_{j_m} M_j^2 (h a_{j_m+1} \varphi_r^{(\infty)}) = 0 \qquad (75)$$

yields from Eq. (72)

$$- M_\infty^2 a_{j_m} a_{j_m+1} \varphi_{i j_m-1} + M_\infty^2 a_{j_m+1} A_2 \varphi_{i j_m} - M_j^2 b_{j_m} A_1 \varphi_{i j_m+1}$$
$$- M_j^2 b_{j_m} b_{j_m+1} \varphi_{i j_m+2} + (M_\infty^2 a_{j_m+1} B_2 - M_j^2 b_{j_m} B_1) = 0. \qquad (76)$$

When we subtract Eqs. (67) we obtain the single equation

$$8\Delta\varphi = \varphi_{i j_m-1} - 9\varphi_{i j_m} + 9\varphi_{i j_m+1} - \varphi_{i j_m+2} - 3h(\varphi_r^{(j)} + \varphi_r^{(\infty)}) \qquad (77)$$

where $\Delta\varphi$ is a known constant which for the final converged solution must agree with the jump at the nacelle trailing edge and at infinity downstream. Eliminating the r derivatives in Eq. (77) by Eqs. (72) leads to

$$(1 + 3a_{j_m}/b_{j_m})\varphi_{i j_m-1} - (9 + 3A_2/b_{j_m})\varphi_{i j_m} + (9 - 3A_1/a_{j_m+1})\varphi_{i j_m+1} \qquad (78)$$
$$- (1 + 3b_{j_m+1}/a_{j_m+1})\varphi_{i j_m+2} - 3(B_1/a_{j_m+1} + B_2/b_{j_m}) - 8\Delta\varphi = 0$$

Equations (76) and (78) are the equations for $j = j_m$ and $j = j_m+1$ required to complete the set of equations for the column relaxation procedure. In this form, the matrix is no longer tridiagonal and more sophisticated methods for solution would be required. However, the tridiagonal matrix is restored by first eliminating $\varphi_{i j_m+2}$ from Eq. (76) and (78) and then eliminating $\varphi_{i j_m-1}$. After simplification, there results

$$[M_j^2 b_{j_m}(3a_{j_m}+b_{j_m}) + M_\infty^2 a_{j_m}(a_{j_{m+1}}+3b_{j_{m+1}})]\,\varphi_{i\,j_m-1}$$
$$-\{9M_j^2 b_{j_m} b_{j_{m+1}} + A_2[3M_j^2 b_{j_{m+1}} + M_\infty^2(a_{j_{m+1}}+3b_{j_{m+1}})]\}\,\varphi_{i\,j_m} \qquad (79)$$
$$+[9M_j^2 b_{j_m} b_{j_{m+1}} + M_j^2 b_{j_m} A_1]\,\varphi_{i\,j_{m+1}}$$
$$+M_j^2 b_{j_{m+1}} B_1 - [3M_j^2 b_{j_{m+1}} + M_\infty^2(a_{j_{m+1}}+3b_{j_{m+1}})]B_2 - 8M_j^2 b_{j_m} b_{j_{m+1}}\Delta\varphi = 0$$

$$[M_\infty^2 a_{j_{m+1}}(A_2 - 9a_{j_m})]\,\varphi_{i\,j_m}$$
$$+\{9M_\infty^2 a_{j_m} a_{j_{m+1}} - A_1[3M_\infty^2 a_{j_m} + M_j^2(3a_{j_m}+b_{j_m})]\}\varphi_{i\,j_{m+1}} \qquad (80)$$
$$-[M_j^2 b_{j_m}(3a_{j_m}+b_{j_m}) + M_\infty^2 a_{j_m}(a_{j_{m+1}}+3b_{j_{m+1}})]\,\varphi_{i\,j_{m+2}}$$
$$+M_j^2 a_{j_{m+1}} B_2 - [3M_\infty^2 a_{j_m} + M_j^2(3a_{j_m}+b_{j_m})]B_1 - 8M_\infty^2 a_{j_m} a_{j_{m+1}}\Delta\varphi = 0$$

Equations (79) and (80) are based on a second order expansion of φ about the streamline points. A simpler first order theory can also be derived. In place of Eqs. (64) we write

$$\varphi^{(\infty)} = \varphi_{i\,j_{m+1}} - \frac{h}{2}\varphi_r\Big|_{r=r_{j_{m+1}}} + O(h^2)$$
$$\varphi^{(j)} = \varphi_{i\,j_m} + \frac{h}{2}\varphi_r\Big|_{r=r_{j_m}} + O(h^2)$$

With φ_r given by Eqs. (65), we have

$$\varphi^{(\infty)} = (3\varphi_{i\,j_{m+1}} - \varphi_{i\,j_{m+2}})/2$$

Similarly,

$$\varphi^{(j)} = (3\varphi_{i\,j_m} - \varphi_{i\,j_{m-1}})/2$$

Substracting these last two equations yields

$$2\Delta\varphi = \varphi_{ij_{m-1}} - 3\varphi_{ij_m} + 3\varphi_{ij_{m+1}} - \varphi_{ij_{m+2}}$$

This relation is simpler than Eq. (67) since it does not contain the first derivative terms. The continuity of slope leads to Eq. (76) for the other equations required to complete the system of column equations. The tri-diagonal form of the system is preserved by first eliminating $\varphi_{ij_{m+2}}$ and then $\varphi_{ij_{m-1}}$, from the two equations. This yields the following two equations in place of Eqs. (79) and (80):

$$-(M_j^2 b_{j_m} b_{j_{m+1}} + M_\infty^2 a_{j_m} a_{j_{m+1}})\varphi_{ij_m} + (3M_j^2 b_{j_m} b_{j_{m+1}} + M_\infty^2 a_{j_{m+1}} A_2)\varphi_{ij_m} - M_j^2 b_{j_m}(3b_{j_{m+1}} + A_1)\varphi_{ij_{m+1}} = (M_j^2 b_{j_m} B_1 - M_\infty^2 a_{j_{m+1}} B_2) - 2M_j^2 b_{j_m} b_{j_{m+1}}\Delta\varphi$$

$$M_\infty^2 a_{j_{m+1}}(A_2 - 3a_{j_m})\varphi_{ij_m} + (3M_\infty^2 a_{j_m} a_{j_{m+1}} - M_j^2 b_{j_m} A_1)\varphi_{ij_{m+1}} - (M_j^2 b_{j_m} b_{j_{m+1}} + M_\infty^2 a_{j_m} a_{j_{m+1}})\varphi_{ij_{m+2}} = (M_j^2 b_{j_m} B_1 - M_\infty^2 a_{j_{m+1}} B_2) + 2M_\infty^2 a_{j_m} a_{j_{m+1}}\Delta\varphi$$

10. Application of the Method of Relaxation to the Solution of the Boundary Value Problem in Figure 3.

In the foregoing analysis, we have formulated the difference equations corresponding to the partial differential equations of Eqs. (9) and (18) for points in the interior of duct and outside stream, for mesh points near the solid boundary, on both sides of the common streamline of the two flows, and near the inlet regions. We have expressed these equations in a form for solving the values of φ along a column of fixed values of i. These equations

J18-047

are non-linear in φ since the quantities u_{ij} and v_{ij} also include the term φ_{ij} . When u_{ij} and v_{ij} are assumed to be fixed and determined by the starting or previously iterated values of φ_{ij} , then the set of equations for the i column is linear in φ_{ij} . The matrix is tridiagonal in form, and is especially easy to solve. Each column is iterated until consecutive approximations of φ_{ij} are within a specified accuracy. For a more complete description of the numerical procedure the reader is referred to the papers by Murman, Cole and Krupp in the referencesat the end of this document.

The required relations for computing the flow field have been presented in sufficient detail in the preceding analysis to set up the procedures for the numerical evaluation of the flow field. In Appendix I, the results of the foregoing analysis will be summarized in a form used directly in the relaxation procedure. In this way, the reader will be able to follow more easily the computer program coded to perform these calculations.

11. Calculation of Streamline Pattern and Duct Mass Flow

The application of the Kutta condition at the nacelle trailing edge requires that φ_x at the fan plane not be arbitrary but be determined as part of the solution for a specified value of M_j far downstream. This is found by requiring that the total mass flow at the duct inlet be equal to the calculated far downstream value. For convenience we prescribe a uniform mass flux distribution at the fan plane and assume that the streamlines far downstream are also parallel. The mass flow rate is then given in terms of φ_x by Eq. (25).

To evaluate the mass flow rate in the free jet far downstream we must

D1 4100 7740 ORIG.3/71

determine the width of the duct flow at this station. Because of the linearized boundary condition and the rectangular mesh, the streamline pattern can be approximated by integrating the flow direction along lines r equal constant (j equal constant in the mesh). Thus

$$R(x) - R_0 = \int_0^x (\phi_{r_1} / \phi_x) dx$$

In terms of the perturbation potential this becomes

$$R(x) - R_0 = \epsilon (M_\infty^2 / M_j^2) \int_0^x \varphi_{r_1} dx$$

The scaled variable r is given in terms of the physical variable r_1, by $r = \tau r_1$. Since $\tau \epsilon = \delta$ we obtain, finally,

$$R(x) - R_0 = \delta (M_\infty^2 / M_j^2) \int_0^x \varphi_r dx \qquad (81)$$

The derivative φ_r at the point r_j is found by fitting a polynomial through the mesh points along the line x_i = constant, differentiating with respect to r and setting $r = r_j$. The integration in x is performed by the trapizoidal rule.

To calculate the mass flow rate far downstream, the quantity m is computed by Eq. (26) for values of $R(x)$ on the boundaries and in the center of the duct flow. Using a polynomial fit, the total mass flow is found by integrating

$$m_t = \int_{R_1}^{R_{j_m}} m \, r \, dr$$

where R_1 and R_{j_m} are the final values of r calculated by Eq. (81) for $i = 1$ and $j = j_m$. With $m = m_t / A_0$

where A_0 is the boundary area of the duct between r_i and r_{j_m}, Eq. (27) yields the appropriate value of φ_x to assign to the inlet for the next iterations. The inlet value of φ_x is updated from time to time until the relaxation converges to suitable accuracy.

12. Examples of Calculated Flows

To demonstrate the operation of the program TEA-343, the configuration described by the coordinates in Tables 1, 2, and 3 was used. The maximum radius of the centerbody wall and the end of the fan cowl and outer duct wall all occur at the axial position x = 1 in the dimensionless variables. The thickness ratio δ used in the parameters K and ϵ was chosen as the increase in centerbody radius from x = 0 to the maximum radius at x = 1 divided by the section length. For the data in Tables 1, 2, and 3, this value is $\delta = 0.15$. For convenience, the boundary value φ_x at x = 0 in the duct was chosen as uniform over the fan plane. The boundary values along x = 0 in the outside stream were chosen to vary with r_1 like $1/(r_1^2+1)^{3/2}$ which is the variation for the incompressible solution fro a source and sink at the axial positions $x = \pm 1$ in a uniform stream given by Milne-Thomson (10) on page 486. With φ_x on the fan cowl at x = 0 given by $C_p = -0.06$ the flow was computed for a Mach number of the exterior stream of $M_{oo} = 0.9$ and a duct far downstream Mach number $M_j = 0.9$. The duct Mach number M_j was increased from $M_j = 0.9$ to 1.25 by increments of .05. Each step required 200 to 300 iterations and complete convergence was not necessarily achieved at each step. It was found that the iterations failed to converge if the first estimate of φ_x at the inlet of the duct was too far from the correct value. A first estimate of φ_x is found by satisfying the conservation of mass flow through the fan plane under the assumption of a uniform flow at Mach

TABLE 1

COORDINATES AND SLOPE OF NACELLE

I	X	R	RUX	DER
1	.010000	1.106185	-.011247	-.001966
2	.030000	1.106106	-.033608	-.005874
3	.050000	1.105950	-.055793	-.009751
4	.076000	1.105632	-.084369	-.014746
5	.110000	1.105020	-.121287	-.021198
6	.154000	1.103906	-.168307	-.029416
7	.204000	1.102206	-.220701	-.038574
8	.254000	1.100052	-.271991	-.047538
9	.308000	1.097228	-.326145	-.057003
10	.360000	1.094032	-.377076	-.065905
11	.410000	1.090527	-.424923	-.074268
12	.460000	1.086608	-.471666	-.082437
13	.510000	1.082286	-.517316	-.090414
14	.560000	1.077570	-.561842	-.098198
15	.604000	1.073102	-.600121	-.104888
16	.638000	1.069449	-.629115	-.109956
17	.664000	1.066540	-.650943	-.113771
18	.688000	1.063768	-.670826	-.117246
19	.710000	1.061154	-.688829	-.120393
20	.730000	1.058718	-.705011	-.123221
21	.750000	1.056225	-.721015	-.126018
22	.770000	1.053677	-.736843	-.128785
23	.790000	1.051074	-.752495	-.131520
24	.810000	1.048417	-.767970	-.134225
25	.830000	1.045705	-.783268	-.136899
26	.850000	1.042941	-.798390	-.139542
27	.870000	1.040124	-.813335	-.142154
28	.890000	1.037255	-.828103	-.144735
29	.910000	1.034335	-.842695	-.147285
30	.930000	1.031364	-.857111	-.149805
31	.950000	1.028343	-.871350	-.152293
32	.970000	1.025272	-.885412	-.154751
33	.990000	1.022153	-.899298	-.157178

TABLE 2

COORDINATES AND SLOPE OF UPPER FAN CONTOUR

I	X	R	RLX	DER
1	.010000	.966365	-.006978	-.001220
2	.030000	.966320	-.018620	-.003254
3	.050000	.966239	-.027177	-.004750
4	.076000	.966099	-.033688	-.005888
5	.110000	.965892	-.034333	-.006001
6	.154000	.965666	-.021931	-.003833
7	.204000	.965601	.010289	.001798
8	.254000	.965902	.061795	.010800
9	.308000	.966832	.139082	.024309
10	.360000	.968516	.234757	.041032
11	.410000	.971041	.346442	.060551
12	.460000	.974627	.477402	.083440
13	.510000	.979441	.627647	.109699
14	.560000	.985653	.797177	.139330
15	.604000	.992407	.950629	.166150
16	.638000	.997799	.847124	.148059
17	.664000	1.001588	.853488	.149172
18	.688000	1.005415	.970308	.169589
19	.710000	1.009321	1.049468	.183425
20	.730000	1.012941	.998243	.174472
21	.750000	1.016193	.870403	.152128
22	.770000	1.019113	.812537	.142014
23	.790000	1.021944	.802480	.140256
24	.810000	1.024615	.709331	.123976
25	.830000	1.026789	.521981	.091231
26	.850000	1.028242	.308549	.053928
27	.870000	1.028963	.118659	.020739
28	.890000	1.029208	.041472	.007248
29	.910000	1.029176	-.096524	-.016870
30	.930000	1.028296	-.409605	-.071590
31	.950000	1.026717	-.422600	-.073861
32	.970000	1.025400	-.520549	-.090981
33	.990000	1.022617	-1.053439	-.184119

COORDINATES AND SLOPE OF LOWER FAN CONTOUR

I	X	R	RX	DER	I	X	R	RX	DER
1	.010000	.577426	-.008413	-.001469	31	.950000	.752259	.389467	.068070
2	.030000	.577372	-.021884	-.003825	32	.970000	.753382	.047770	.008349
3	.050000	.577278	-.030930	-.005406	33	.990000	.752668	-.313396	-.054775
4	.076000	.577123	-.036058	-.006302	34	1.010000	.751912	-.171175	-.029918
5	.110000	.576916	-.031456	-.005498	35	1.030000	.751319	-.168127	-.029385
6	.154000	.576757	-.006473	-.001131	36	1.050000	.750736	-.165322	-.028895
7	.204000	.576918	.047973	.008385	37	1.076000	.749992	-.162040	-.028321
8	.254000	.577676	.130138	.022745	38	1.110000	.749041	-.158368	-.027679
9	.308000	.579444	.250010	.043697	39	1.154000	.747838	-.154659	-.027031
10	.360000	.582357	.396011	.069213	40	1.204000	.746500	-.151873	-.026544
11	.410000	.586535	.564650	.098689	41	1.256000	.745126	-.150588	-.026320
12	.460000	.592307	.761019	.133010	42	1.308000	.743757	-.150947	-.026382
13	.510000	.599916	.985106	.172176	43	1.360000	.742378	-.152950	-.026732
14	.560000	.609605	1.236913	.216186	44	1.415000	.740890	-.156858	-.027415
15	.604000	.620047	1.494805	.261260	45	1.475000	.739214	-.163218	-.028527
16	.638000	.630228	1.947037	.340301	46	1.540000	.737309	-.172579	-.030163
17	.664000	.639757	2.217422	.387558	47	1.610000	.735121	-.185532	-.032427
18	.688000	.649441	2.426947	.424179	48	1.690000	.732403	-.203985	-.035652
19	.710000	.659386	2.751118	.480837	49	1.780000	.729000	-.229395	-.040093
20	.730000	.669363	2.929592	.512031	50	1.880000	.724711	-.261448	-.045696
21	.750000	.679715	2.988437	.522315	51	2.000000	.718836	-.298449	-.052162
22	.770000	.690247	3.036574	.530729	52	2.150000	.710435	-.341914	-.059763
23	.790000	.700917	3.049077	.532914	53	2.350000	.697537	-.395136	-.069061
24	.810000	.711351	2.888728	.504888	54	2.600000	.678955	-.453958	-.079342
25	.830000	.720895	2.549199	.445546	55	2.900000	.653544	-.513279	-.089710
26	.850000	.729137	2.165191	.378429	56	3.250000	.620457	-.561451	-.098130
27	.870000	.736056	1.813341	.316933	57	3.650000	.582300	-.506648	-.088551
28	.890000	.741988	1.605641	.280632	58	4.050000	.552897	-.311041	-.054363
29	.910000	.747138	1.281976	.224062	59	4.450000	.542035	0.000000	0.000000
30	.930000	.750565	.665012	.116230					

TABLE 3

number M_j through the fan exit plane at the trailing edge of the fan cowl (Fig.1), and the program corrects this value during the computations.

The distributions of pressure coefficient on the centerbody and on the duct flow outer boundary are presented in Fig. 6 for $M_j = 1.2$. The coefficients are based on the exterior free stream dynamic pressure. The velocity is seen to be highest and the pressure coefficient lowest at the point of maximum centerbody radius x = 1. The streamline pattern of this flow is shown in Figure 7. The duct flow is accelerated to supersonic velocities leading to the sharply curved sonic line terminating close to the fan cowl trailing edge. Note that the flow near the centerbody is rapidly decelerated by a shock resulting in a small local region of subsonic flow.

Figure 8 shows the pressure distribution on the centerbody and duct flow free streamline for a duct Mach number of $M_{\infty} = 1.25$. For this value of the Mach number, the duct flow remains supersonic downstream of the curved sonic line as seen in Figure 9. The flow decelerates from the maximum value at x = 1 but does not become subsonic. The streamline pattern is very similar to that for $M_{\infty} = 1.20$.

The centerbody of Figure 9 was extended downstream as shown in the streamline pattern of Figure 10 (See Table 3). This corresponds more closely to the actual flow conditions and the resulting pressure distribution shown in Figure 11 is similar to that of Figure 8 in the vicinity of the fan exit plane.

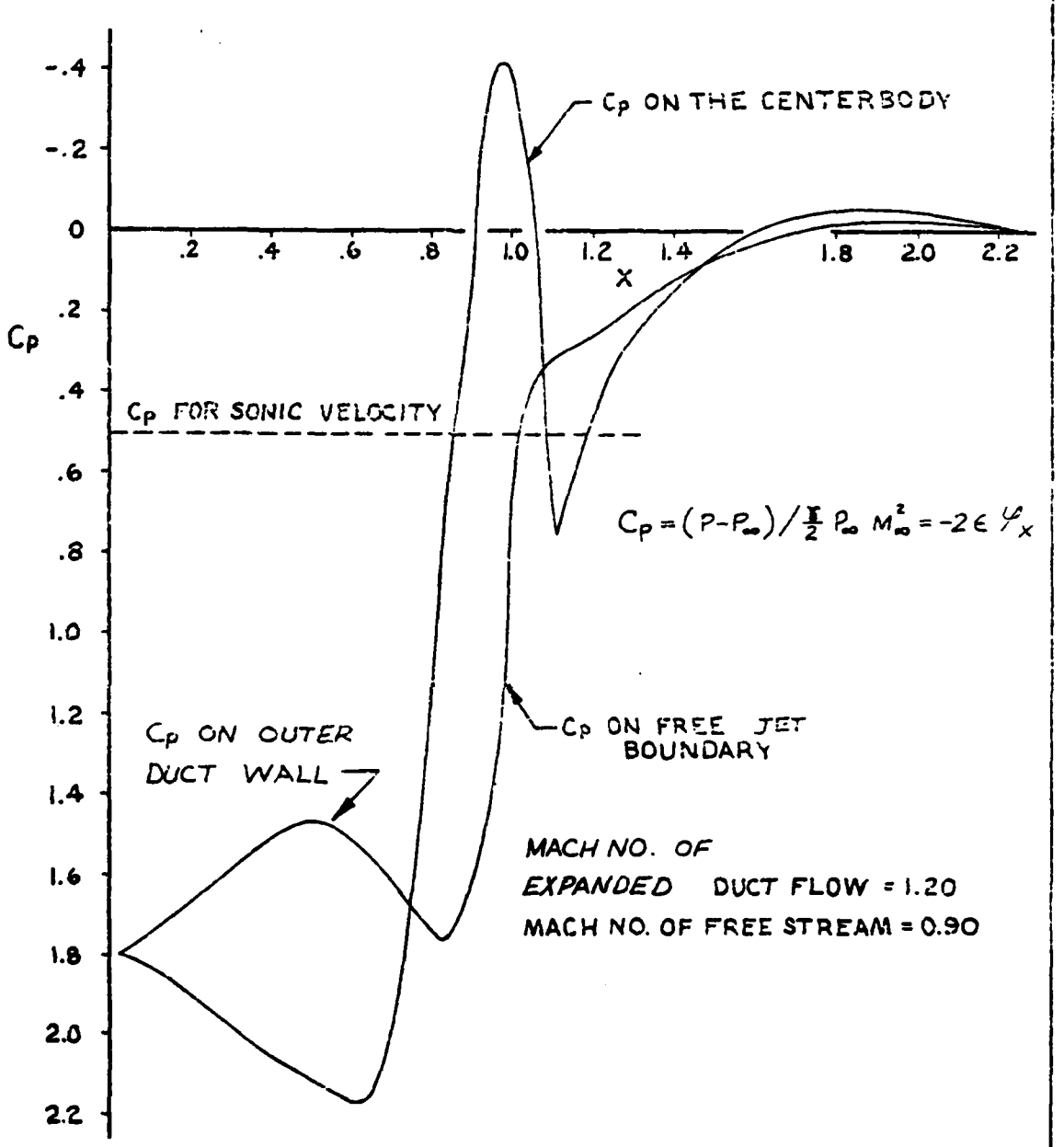

FIGURE 6 DISTRIBUTION OF THE PRESSURE COEFFICIENTS ON THE CENTERBODY AND FREE STREAMLINE BOUNDARY. PRESSURE COEFFICIENT IS BASED ON THE DYNAMIC PRESSURE OF FREE STREAM.

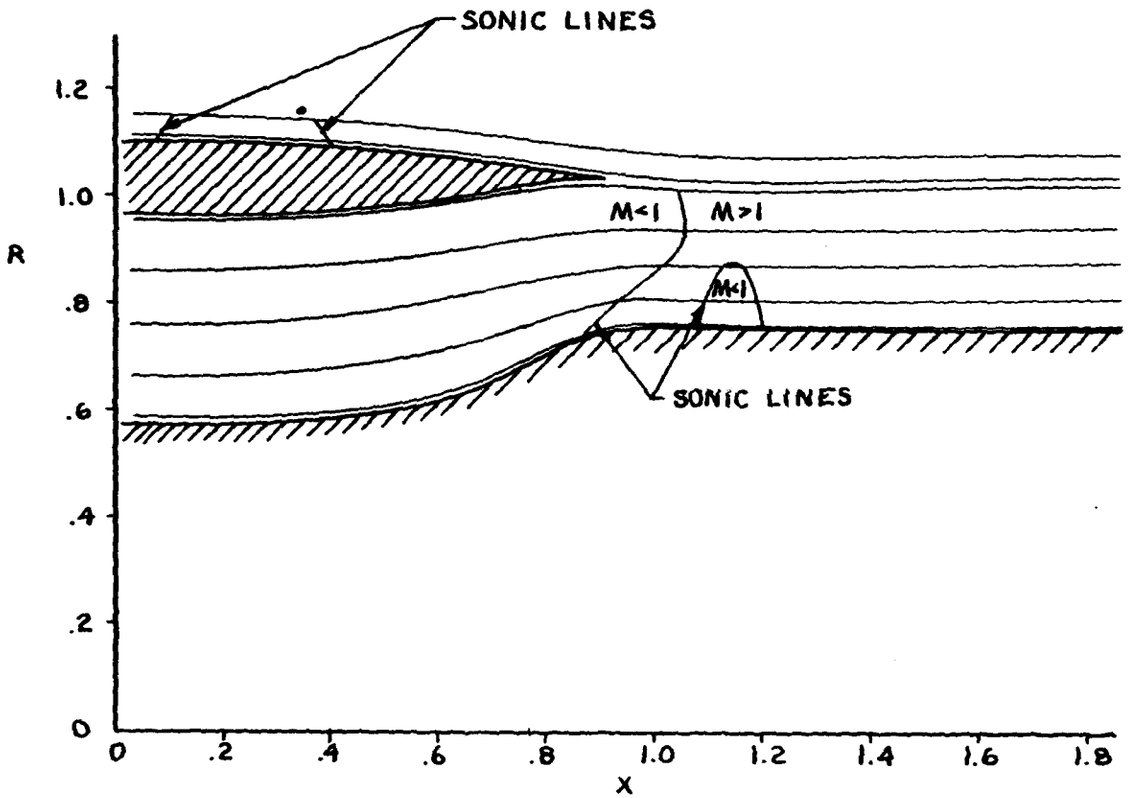

FIGURE 7 STREAMLINE PATTERN IN THE FAN DUCT WITH SONIC LINES FOR FLOW CONDITIONS OF FIGURE 6. NOTE IMBEDED REGION OF SUBSONIC FLOW NEAR CENTERBODY DOWNSTREAM OF SONIC LINE

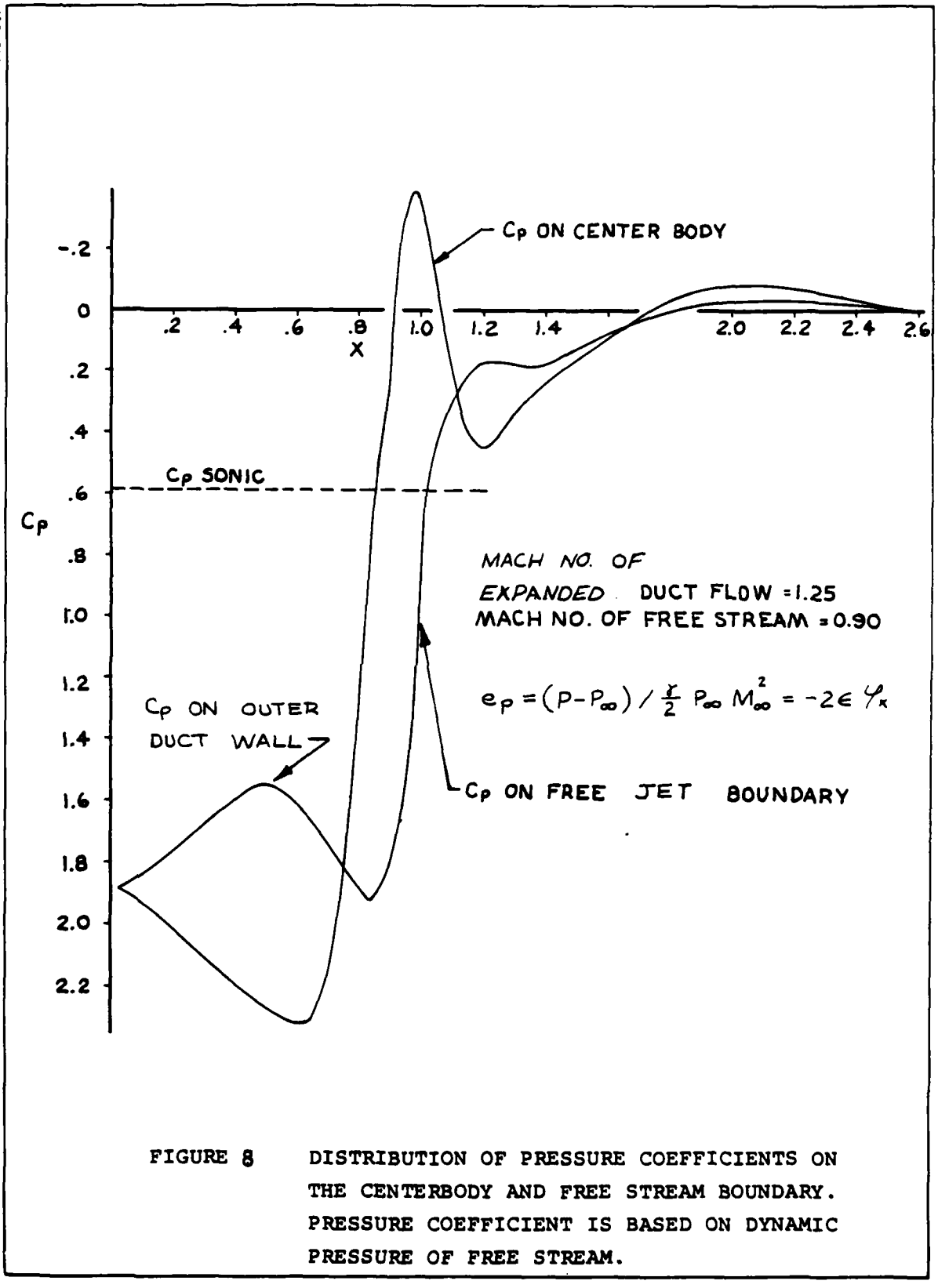

FIGURE 8 DISTRIBUTION OF PRESSURE COEFFICIENTS ON THE CENTERBODY AND FREE STREAM BOUNDARY. PRESSURE COEFFICIENT IS BASED ON DYNAMIC PRESSURE OF FREE STREAM.

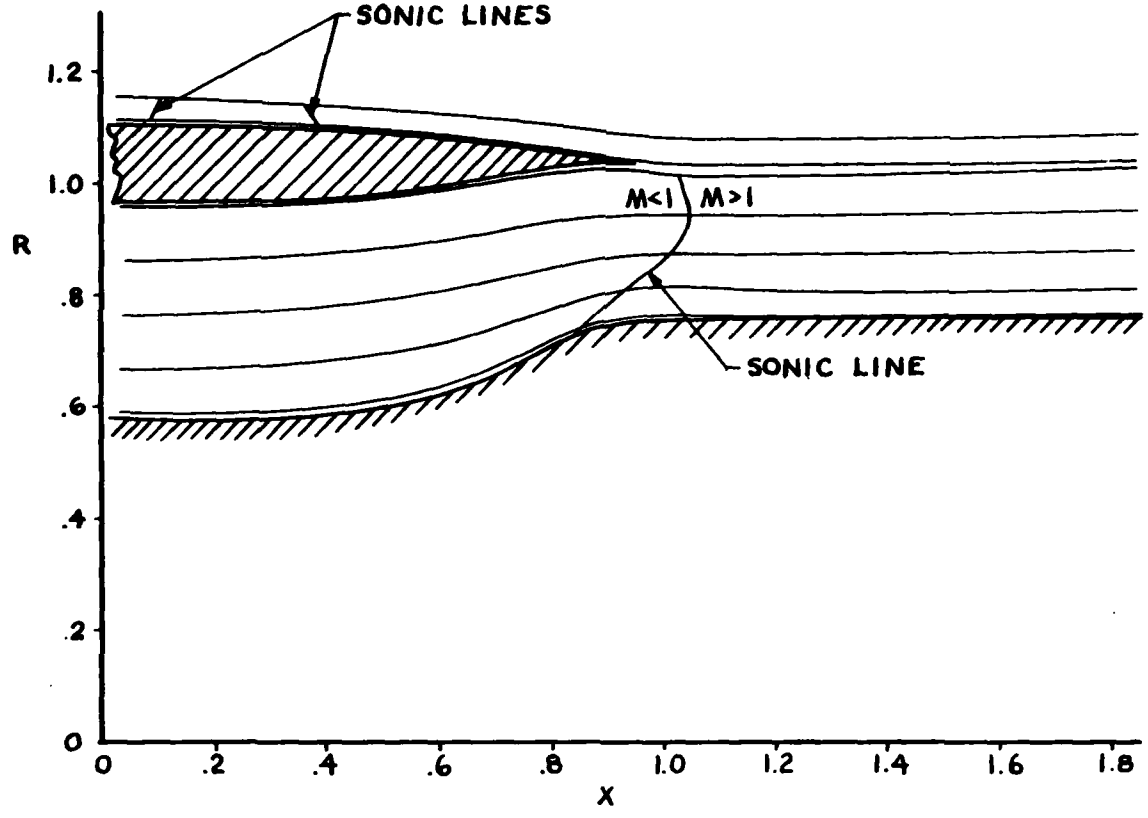

FIGURE 9 STREAMLINE PATTERN IN THE FAN DUCT WITH SONIC LINES FOR FLOW CONDITIONS OF FIGURE 8

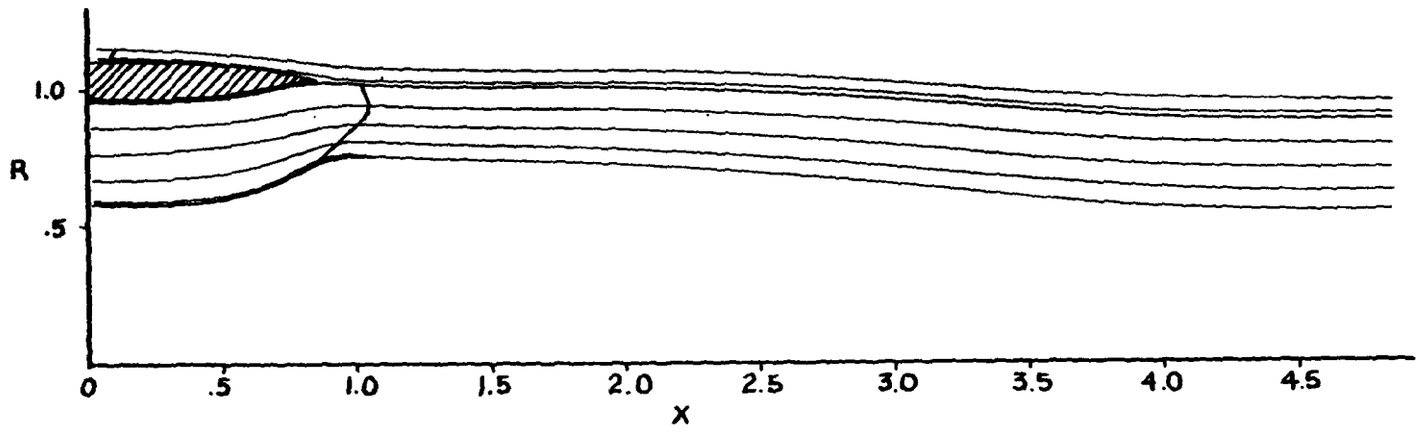

FIGURE 10 STREAMLINE PATTERN FOR THE EXTENSION OF THE CENTERBODY OF FIGURE 8 TO CORRESPOND TO MORE REALISTIC FLOW

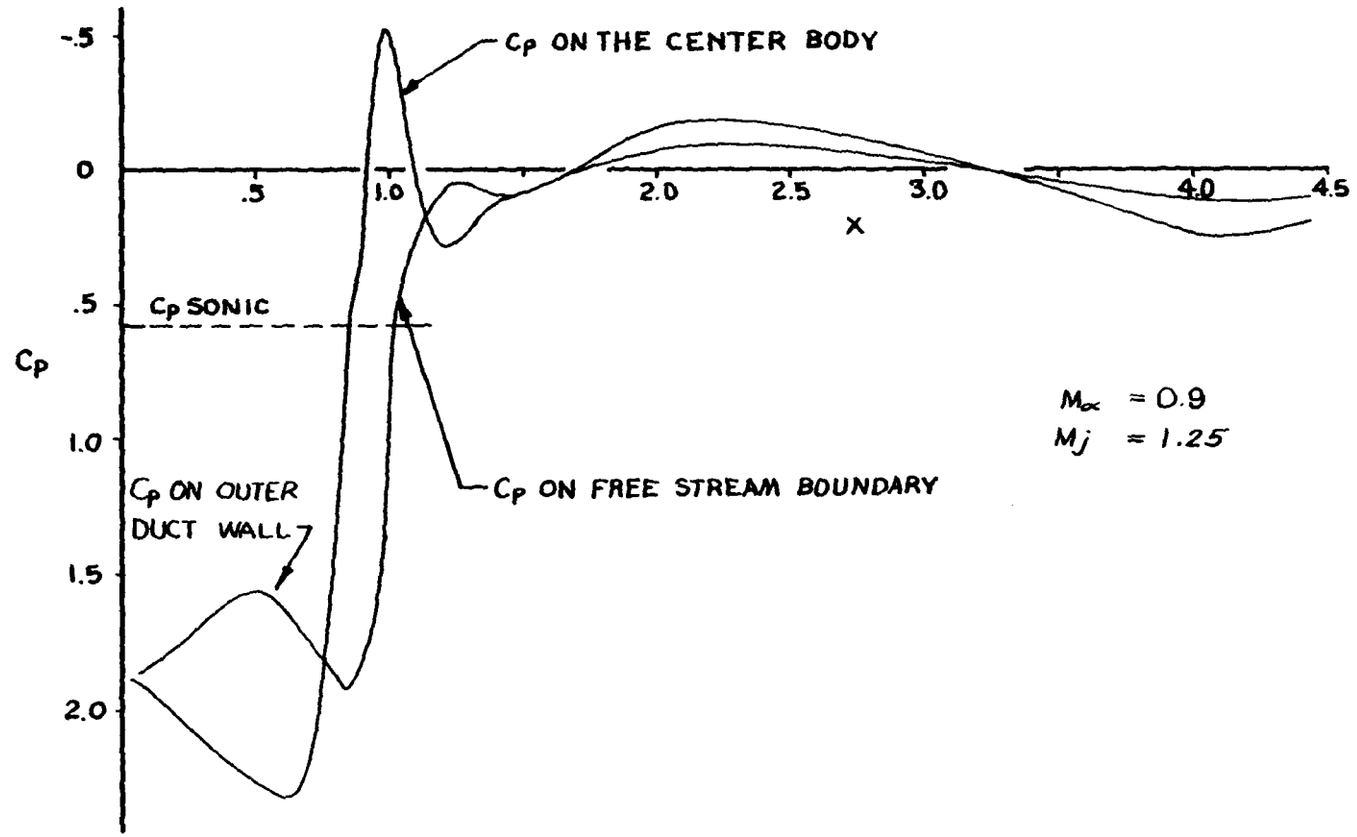

FIGURE 11 DISTRIBUTION OF PRESSURE COEFFICIENTS ON THE CENTERBODY AND FREE STREAM BOUNDARY OF FIGURE 10

APPENDIX I: SUMMARY OF THE EQUATIONS USED IN THE COMPUTER PROGRAM TRANSDUCT

The equations to be solved at each column i have been expressed in a form which yields a tridiagonal N x N matrix for the coefficients of the variables, where N is the number of values of φ in a single column. The elements of the matrix are described by three N dimensional vectors. The coefficient of the diagonal term φ_{ij} in the J^{th} equation is the component of the vector denoted by

DIAG(J)

in the program. The vector of coefficients of $\varphi_{i\,j+1}$ to the right of the diagonal is designated as

SUPER(J)

while the vector of coefficients to the left of the diagonal $\varphi_{i\,j-1}$ is designated by

SUB(J)

1. Coefficients Based on the Mesh Points

When the distributions of the x_i and r_j are established, the coefficients depending upon these quantities can be determined once and for all at the ouset of computations. For the x coordinate, we define

$$
\begin{aligned}
c_1 &= 1/(x_2^2 - x_1^2) \\
c_i &= 1/(x_{i+1} - x_i)\,(x_{i+1} - x_{i-1}) \\
d_1 &= 1/(x_2 + x_1) \\
d_i &= 1/(x_i - x_{i-1})\,(x_{i+1} - x_{i-1}) \\
c_{11} &= 1/2(x_2 - x_1), c_{1i} = (x_i - x_{i-1})\,c_i \\
d_{11} &\ 1/2, d_{1i} = (x_{i+1} - x_i)\,d_i
\end{aligned}
\tag{81}
$$

For the r coordinate, we obtained

$$a_1 = 0$$

$$a_j = (r_j + r_{j-1})/2\, r_j\, (r_{j+1} - r_{j-1})\, (r_j - r_{j-1}) \qquad j > 1$$

$$b_j = (r_j + r_{j+1})/2\, r_j\, (r_{j+1} - r_{j-1})\, (r_{j+1} - r_j) \qquad j \geq 1$$

The value of b_1 follows the preceding formula for $r_0 = 2r_b - r_1$, where r_b is the mean scaled radius of the inner duct wall. All the preceding coefficients are computed in the subroutine MESH.

2. The Vectors: SUB, DIAG, SUPER, and RHS

In the mesh for the boundary value problem described in Figure 2, we define the maximum number of r = constant lines by JMX (j_{max}) and the maximum number of x = constant lines by IMX (i_{max}). For I < IO, the flow field is divided into a duct flow and the outside flow over the nacelle which are solved separately in the relaxation process. The number of points along constant x_i inside the duct is JM (j_m in the text).

The vectors, SUB, DIAG, and SUPER are N dimensional, where N is the number of points in a column. The vector components are identified in such a way that

SUPER(N) = SUB(1) = 0;

Thus, the J^{th} equation for each I is seen to be described by a FORTRAN statement of the form

SUB(J)*P(I,J-1) + DIAG(J)*P(I,J) + SUPER(J)*P(I,J+1) = RHS(J) (82)

where P(I,J) = $\varphi_{i\,j}$ and RHS denotes the right hand side terms of the equations. The subroutine TRISOL which solves the tridiagonal system then is called by a statement of the form

CALL TRISOL(SUB,DIAG,SUPER,RHS,PHI,AUX,N) (83)

The quantity PHI is the vector solution of P(I,J) for fixed I in the set of equations described by Equation (82), AUX is an N vector of storage required by the program. By comparing Equation (82) with the equations in the analysis one can write down the formulae for the vector components of SUB, DIAG, SUPER, and RHS.

The quantity IO, (i_0 in the text) denotes the line x = constant of the mesh which intersects the nacelle line of Figure 2 nearest the trailing edge. For all values of $i \leq i_0$, the column set of equations is divided into two parts, the duct flow and outside stream; and the two sections of the column are solved separately in the relaxation process. For $i > i_0$, the entire column encompassing both flows is solved simultaneously.

3. Formulation of the Column Equations

Because of the initial condition

$$\varphi_x = f(r) \tag{84}$$

at x = 0, the column i = 1 is a special case. From comparison of Equation (82) with Equation (60), we have

$$\begin{aligned}
&SUB(J) = a_j && j = 2 \text{ to } j_m \\
&SUPER(J) = b_j && j = 1 \text{ to } j_m - 1 \\
&DIAG(J) = -(v_{1j}c_1 + a_j + b_j) && j = 2 \text{ to } j_m - 1 \\
&RHS(J) = -v_{1j}\,(c_1 \varphi_{2j} - d_1 f_j) && j = 2 \text{ to } j_m - 1 \\
&SUPER(JM) = 0
\end{aligned} \tag{85}$$

where $f_j = f(r_j)$ and

$$v_{1j} = (1-M_j^2)k/(1-M_\infty^2) - (\gamma + 1)\left[c_{11}(\varphi_{2j} - \varphi_{1j}) + d_{11}f_j\right] \tag{86}$$

By comparison of Equation (82) with Equations (45) and (49) we obtain

$$\begin{aligned} DIAG(1) &= -(v_{11}c_1 + b_1) \\ RHS(1) &= -v_{11}(c_1\varphi_{21} - d_1 f_1) + \alpha_1 R'(x_1) \\ DIAG(JM) &= -(v_{1j_m}c_1 + a_{j_m}) \\ RHS(JM) &= -v_{1j_m}(c_1\varphi_{2j_m} - d_1 f_{j_m}) - \alpha_2 R'(x_1) \end{aligned} \tag{87}$$

where $\alpha_1 = M_j^2 r_b / M_\infty^2 r_1 (r_2 - r_0)$

and $\alpha_2 = M_j^2 r_{j_m+1/2} / M_\infty^2 r_{j_m}(r_{j_m+1} - r_{j_m-1})$ (88)

The JM-1 values of φ_{ij} are solved by TRISOL and iterated. For i = 1 and $j_m < j < j_{max}$, we obtain similar relations. For J = 1 to JMX1 - JM = JMX-1-JM, we define the vectors for the column above the nacelle as

$$\begin{aligned} SUB(J) &= a_{j_m+j} \qquad SUB(1) = 0 \\ SUPER(J) &= b_{j_m+j} \\ DIAG(J) &= -(u_{i_{j_m+j}}c_1 + a_{j_m+j} + b_{j_m+j}) \\ RHS(J) &= -u_{i_{j_m+j}}(c_1\varphi_{2j_m+j} - d_1 f_{j_m+j}) \end{aligned} \tag{89}$$

and

$$SUPER(JMX1-JM) = 0$$

$$\begin{aligned} DIAG(1) &= -(u_{i_{j_m+1}}c_1 + b_{j_m+1}) \\ RHS(1) &= -u_{i_{j_m+1}}(c_1\varphi_{2j_m+1} - d_1 f_{j_m+1}) + \alpha_3 R'_u(x_1) \end{aligned} \tag{90}$$

where $u_{ij} = \kappa - (\gamma+1)[c_{ij}(\varphi_{2j} - \varphi_{ij}) + d_{ij} f_j]$ (91)

and

$$\alpha_3 = r_{jm+1/2}/r_{jm+1}\,(r_{jm+2} - r_{jm})$$

Since only subsonic inlet conditions will be prescribed, the case u_{1j} and $v_{1j} < 0$ is not considered.

4. Formulation of the Column Equations $2 \leq i \leq i_0$

For $1 < i \leq i_0$ and inside the duct, we have from the comparison of Equation (82) with Equations (39), (45), and (49), when $v_{ij} > 0$,

$$\begin{aligned}
&SUB(J) = a_j && j = 2 \text{ to } j_m \\
&SUB(1) = 0 \\
&SUPER(J) = b_j && j = 1 \text{ to } j_m - 1 \\
&SUPER(JM) = 0 \\
&DIAG(J) = -(v_{ij}\, e_i + a_j + b_j) && j = 2 \text{ to } j_m - 1 \\
&RHS(J) = -v_{ij}(e_i \varphi_{i+1j} + d_i \varphi_{i-1j}) && j = 2 \text{ to } j_m - 1 \\
&DIAG(1) = -(v_{i1}\, e_i + b_1) \\
&RHS(1) = -v_{i1}(c_i \varphi_{i+1,1} + d_i \varphi_{i-1,1}) + \alpha_1 R'(x_i) \\
&DIAG(JM) = -(v_{ij_m}\, e_i + a_{j_m}) \\
&RHS(JM) = -v_{ij_m}(c_i \varphi_{i+1j_m} + d_i \varphi_{i-1j_m}) - \alpha_2 R'_L(x_i)
\end{aligned} \tag{92}$$

By comparison of Equation (82) with Equations (41), (46), and (50), we have for the supersonic flow, $v_{ij} < 0$ and $v_{i-1\,j} < 0$, the following terms in place of the ones above:

$$\begin{aligned}
&DIAG(J) = v_{i-1} c_{i-1} - a_j - b_j, && 2 < j < j_m - 1 \\
&RHS(J) = v_{i-1j}(e_{i-1} \varphi_{i-1j} - d_{i-1} \varphi_{i-2j}), && 2 < j < j_m - 1
\end{aligned} \tag{93}$$

$$
\begin{aligned}
\text{DIAG}(\ ) &= v_{i-1j}\, c_{i-1} - b_1 \\
\text{RHS}(1) &= v_{i-1j}\,(e_{i-1}\varphi_{i-1,1} - d_{i-1}\varphi_{i-2,j}) + \alpha_1 R'(x_i) \\
\text{DIAG}(JM) &= v_{i-1j_m}\, c_{i-1} - a_{j_m} \\
\text{RHS}(JM) &= v_{i-1j_m}\,(e_{i-1}\varphi_{i-1j_m} - d_{i-1}\varphi_{i-2j_m}) - \alpha_2 R'(x_i)
\end{aligned}
$$

For $1 < i \leq i_0$ in the exterior flow over the nacelle we have, analogous to Equations (92) and (93),

$$
\begin{aligned}
\text{SUB}(J) &= a_{j+j_m} \qquad 2 < j < j_{max} - j_m - 2 \\
\text{SUB}(1) &= 0 \\
\text{SUPER}(J) &= b_{j+j_m} \\
\text{SUPER}(JMX\text{-}JM\text{-}1) &= 0 \\
\text{DIAG}(J) &= -(u_{ij+j_m} + a_{j+j_m} + b_{j_m+J}), \quad 2 \leq j \leq j_{max} - j_m - 1 \\
\text{RHS}(J) &= -u_{ij+j_m}(c_i \varphi_{i+1\, j+j_m} + d_i \varphi_{i-1\, j_m}), \quad 2 \leq j \leq j_{max} - j_m - 1
\end{aligned}
\tag{94}
$$

For comparison of Equation (82) with Equation (51) we have

$$
\begin{aligned}
\text{DIAG}(1) &= -(u_{ij_m+1}\, e_i + b_{j_m+1}) \\
\text{RHS}(1) &= -u_{ij_m+1}(c_i \varphi_{i+1,j_m+1} + d_i \varphi_{i-1,j_m+1}) + \alpha_3 R'(x_i)
\end{aligned}
$$

where $\alpha_3 = r_{j_m+1/2} / r_{i_m+1}\,(r_{j_m+2} - r_{j_m})$. The hyperbolic case $u_{ij} < 0$ can be written down by following the pattern of Equations (92) and (93). The equations, JMX-JM-1 in number, are solved independently of the duct flow.

5. Formulation of the Column Equations $i > i_0$

For $i > i_0$, the points are downstream of the trailing edge of the nacelle and the entire column of equations to be solved simultaneously encompasses both the duct and exterior flow. For all points except

$j = 1$, j_m, and j_m+1, we have

$$\begin{aligned} &SUB(J) = a_j \qquad && SUB(1) = 0 \\ &SUPER(J) = b_j \qquad && SUPER(JMX-1) = 0 \end{aligned} \tag{95}$$

For $j < j_m$,

$$\begin{aligned} DIAG(J) &= -(v_{ij}\, e_i + a_j + b_j) \quad \text{for } v_{ij} > 0 \\ &= (v_{i-1j} c_{i-1} - a_j - b_j) \quad \text{for } v_{ij} < 0 \\ RHS(J) &= -v_{ij}\, (c_i \varphi_{i+1j} + d_i \varphi_{i-1_j}) \quad \text{for } v_{ij} > 0 \\ &= v_{i-1j}\, (e_{i-1} \varphi_{i-1j} - d_{i-1} \varphi_{i-2j}) \quad \text{for } v_{ij} < 0 \end{aligned} \tag{96}$$

For $j > j_m - 1$,

$$\begin{aligned} DIAG(J) &= -(u_{ij} e_i + a_j + b_j) \quad \text{for } u_{ij} > 0 \\ &= (u_{i-1j} c_{i-1} - a_j - b_j) \quad \text{for } u_{ij} < 0 \\ RHS(J) &= -u_{ij}\, (c_i \varphi_{i+1j} + d_i \varphi_{i-1j}) \quad \text{for } u_{ij} > 0 \\ &= u_{i-1j}\, (c_{i-1} \varphi_{i-1j} - d_{i-1} \varphi_{i-2j}) \quad \text{for } u_{ij} < 0 \end{aligned} \tag{97}$$

For the lower boundary condition we have

$$\begin{aligned} DIAG(1) &= -(v_{i1}\, e_i + b_1) \quad \text{for } v_{i1} > 0 \\ &= v_{i-11}\, c_{i-1} - b_1 \quad \text{for } v_{i1} < 0 \\ RHS(i) &= -v_{i1}\, (c_i \varphi_{i+1,1} + d_i \varphi_{i-1,1}) + \alpha_1 R'(x_i) \quad \text{for } v_{i1} > 0 \\ &= v_{i-1}\, (e_{i-1} \varphi_{i-1,1} - d_{i-1} \varphi_{i-2,1}) + \alpha_1 R'(x_i) \quad \text{for } v_{i1} < 0 \end{aligned}$$

The calculation of the vector components for JM and JM+1 resulting from the boundary conditions on the free streamline are somewhat more complicated. Let $\overline{DIAG(JM)}$ and $\overline{DIAG(JM+1)}$ denote the quantities computed from Equations (96) and (97), respectively. Then from Equations (73) and (74) we see that

$$\begin{aligned} A_1 &= \overline{DIAG(JM+1)} + a_{jm+1} \\ B_1 &= -\overline{RHS(JM+1)} \end{aligned}$$

$$A_2 = -\overline{DIAG(JM)} - b_{jm} \qquad (98)$$
$$B_2 = \overline{RHS(JM)}$$

Let $g_1 = M_j^2 (3a_{j_m} + b_{j_m})$

$$g_2 = M_\infty^2 (a_{j_m+1} + 3b_{j_m+1}) \qquad (99)$$

$$g_3 = M_j^2 b_{j_m+1}$$

and

$$G_1 = b_{j_m+1} g_1 + a_{j_m} g_2 \qquad G_6 = M_\infty^2 a_{j_m+1}$$

$$G_2 = 9b_{j_m} g_3 \qquad G_7 = 8M_j^2 b_{j_m} b_{j_m+1}$$

$$G_3 = 3g_3 + g_2 \qquad G_8 = M_j^2 b_{j_m} \qquad (100)$$

$$G_4 = 9a_{j_m} G_6 \qquad G_9 = 8M_\infty^2 a_{j_m} a_{j_m+1}$$

$$G_5 = 3M^2 a_{j_m} + g_1$$

Then for JM and JM+1 we have

$$SUB(JM) = G_1$$
$$DIAG(JM) = -(G_2 + G_3 A_2)$$
$$SUPER(JM) = G_2 + G_8 A_1 \qquad (101)$$
$$RHS(JM) = -G_8 B_1 + G_3 B_2 + G_7 \Delta\varphi$$
$$SUB(JM+1) = G_6 A_2 - G_4$$
$$DIAG(JM+1) = G_4 - G_5 A_1$$
$$SUPER(JM+1) = -G_1$$
$$RHS(JM+1) = G_9 \Delta\varphi - G_6 B_2 + G_5 B_1$$

The G_j constants are computed once and for all at the beginning of calculations by the subroutine MESH.

APPENDIX II: INSTRUCTIONS FOR USE OF THE PROGRAM TRANSDUCT

1. The Input Data Cards

The parameters required by the program are read in by a namelist called PARAM. These parameters are designated by the notation listed and defined below:

Namelist	PARAM
LSERES	Series number of the flow configuration.
LRUN	Run number of the series.
XMA	Mach number of undisturbed exterior stream.
XMJ	Mach number of expanded fan jet flow far downstream. When starting from an initial parallel flow (MODIN = 1), XMJ must be less than one for the solution to converge. If a supersonic value of XMJ is required, then a sequence of solutions with XMJ incremented by .05 or .1 must be run until the value of XMJ is reached.
NMAX	Maximum number of iterations to be computed. This is chosen on the basis of maximum computing time allowed for each run and is discussed at the end of this section.
JMX	Total number of radial grid points defining the mesh (j index). JMX = 41 for the examples described in the report.
IMX	Total number of axial grid points defining the mesh (i index). IMX = 60 for the examples described in the report.
IO	Index for the value of x nearest the trailing edge of the fan cowl. Grid must be constructed so that trailing edge lies at midpoint between grid points X(IO) and X(IO + 1). IO is 33 for the computed examples in the report.
JM	Index of largest radial mesh variable in the duct flow. JM = 20 in the example flows.
MODIN	If MODIN = 1, potential field is initialized for uniform flow. If MODIN = 2, potential field from cards punched on a previous run is read for the initial potential field, P(I,J).
MODOUT	If MODOUT = 2, the potential field from the solution is punched on cards. If MODOUT = 1, no data is punched.

Namelist	PARAM
Linear	If TRUE (T), the linearized subsonic flow is computed. If FALSE (F), the complete non-linear transonic small perturbation equations are solved.
W1	Over-relaxation parameter for subsonic columns. A value of 1.4 is suggested. However, it may vary between 1 and 1.9, but larger values than 1.4 may lead to divergence of the solution.
CPNAC	Coefficient of pressure on the fan cowl at left boundary of Fig. 2 for computing φ_x which in the present formulation must be restricted to subsonic values. This number is usually taken from experimental measurements. The remaining values along x = 0 in the outside stream are computed to vary like $1/(r_1+1)^{3/2}$. This is the same as the incompressible solution from a source and sink at x = ± 1. (see p. 486, Sec. 16-26 of Milne-Thomson (10)). This formulation was chosen for simplicity and convenience and should give a fair distribution for most calculations.
NA	Number of iterations between updating of φ_x value at duct input. When the number is large, the solutions may later start to diverge if φ_x value is not correct. Suggested values are 20 to 100.
PXIN	Starting inlet value of φ_x at the fan plane. In the present form of the program the distribution of φ_x is uniform across the fan plane. This value is updated every NA iterations when WPX > 0. A first estimate is required and a reasonable value is obtained from Eq. (27) using $m = A_f/A_e$ with the aid of Eqs. (11), (16), and (17) to determine K_1. The quantity A_f is the duct area of the fan plane and A_e is the area of the duct at the transverse plane through the fan cowl trailing edge.
DRFAC	Stretching factor for adjacent mesh increments in radial direction. Used for expanding the mesh in the far field where the flow does not change rapidly. DRFAC must satisfy the inequality: $1 \leq$ DRFAC < 2. Values of 1.15 and 1.2 were used in the examples in the report. Its value is determined by how many points are in the grid and how far mesh is to be extended.
ERR	Maximum error allowed for convergence. If the maximum difference between two iterated values of φ becomes less than ERR, the computation is terminated; otherwise, the program is terminated after NMAX iterations. Suggested value for ERR is 0.0001.

Namelist	PARAM
WPX	Factor for updating φ_x at duct inlet. $0 \leq$ WPX ≤ 1. If WPX = 0, then old value is retained. If WPX = 1, then new value computed from mass flow far downstream of duct is used. WPX = 1/2 updates with the arithmetic mean of former and newly computed values. Until one observes how the updated values change every NA iteration, the value of 1/2 is a safe value for starting.
NP	Number of iterations between intermediate printout.

A typical set of PARAM data cards is presented below. Each card is punched starting in column 2.

```
$PARAM                  MODOUT=1,
LSERES=5,               MODOUT=2,
LRUN=1,                 LINEAR=.T.,
XMA=0.8,                LINEAR=.F.,
XMJ=0.85,               W1=1.3,
NMAX=400,               CPNAC=-0.06,
JMX=41,                 NA=10,
IMX=60,                 PXIN=-1.21,
IO 33,                  DRFAC=1.15,
JM=15,                  ERR=0.0001,
MODIN=2,                NP=20,
MODIN=1,                $END
```

For the parameters MODIN, MODOUT, and LINEAR, the last of each pair of cards read is the information used by the program. Also, more than one parameter may be punched on a single card. A space must be left between the comma and the next parameter name.

After the PARAM list is read, then a single card with 12 integers punched according for FORMAT (12I4) is read. These are index values of the x grid at which intermediate values of φ and φ_x are printed out every NP iteration.

The coordinates for the duct and nacelle boundaries are read by the subroutine BODY along with the axial coordinates for the mesh points. If MODIN in the parameter list is set equal to 2, then the cards for P(I,J), the values of φ at the mesh points from a previous run must be included at the end of those data cards read in by the subroutine BODY.

In summary, the data deck for the program consists of the following (see Figures 12 and 13):

1) Title card: TRANSDUCT.

2) End of record card (6,7,8 punches in column 1).

3) PARAM cards.

4) Card for the twelve intermediate values of the x index for which intermediate values of the potential φ and the derivative φ_x are printed every NP times. Card FORMAT is 12I4.

5) Coordinates of the x grid points. Punched on cards according to the FORMAT 10F8.6.

6) Deck of boundary data cards. The make up of this deck will depend upon how contours are defined and data are read by the subroutine BODY (see Figure 13).

7) For MODIN=2, the φ grid values punched from a previous run must be included.

For the computed examples described in this report, the running time was 0.61 seconds on the CDC 6600 for each iteration with 41 X 60 = 2460 grid points. Since the number of computer operations is almost directly proportional to the number of grid points, then the running time can quickly be estimated for grids with more or less points than 2460.

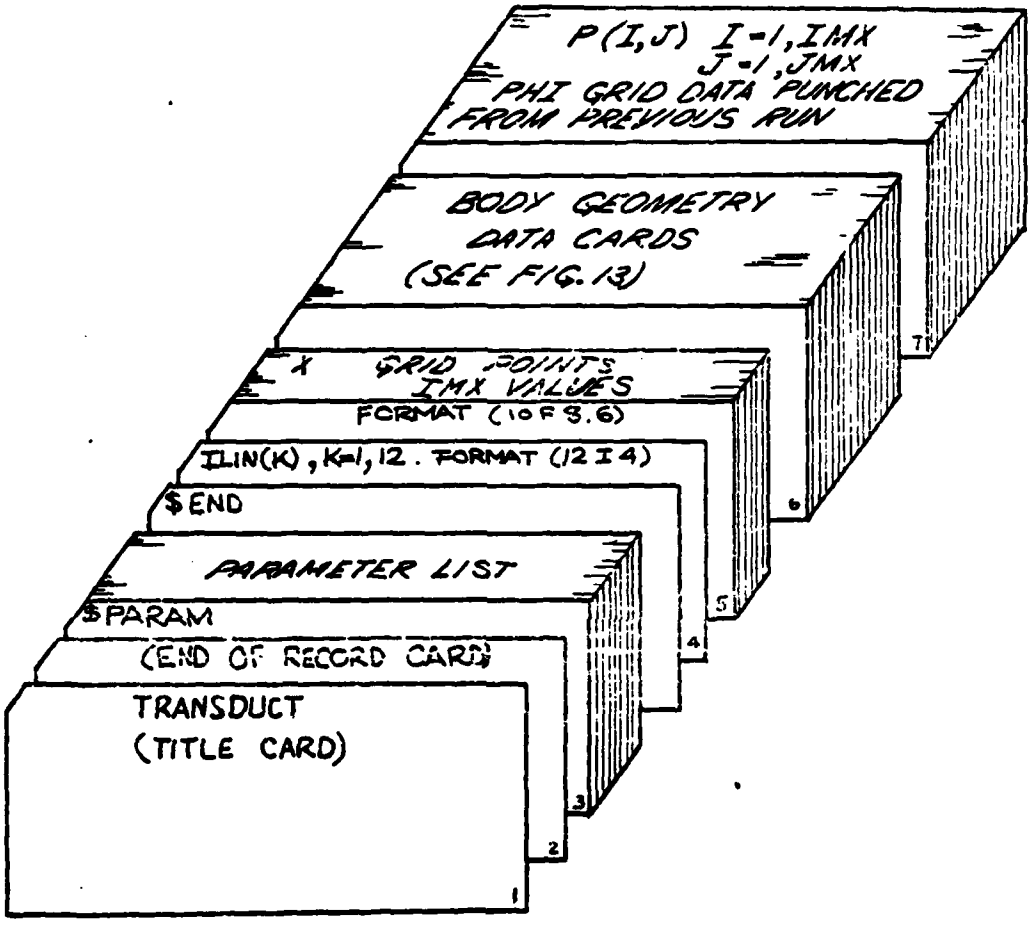

FIGURE 12 ILLUSTRATION OF THE DATA CARDS REQUIRED BY THE PROGRAM FOR MODIN = 2. FOR MODIN = 1, P(I,J) DECK IS OMITTED.

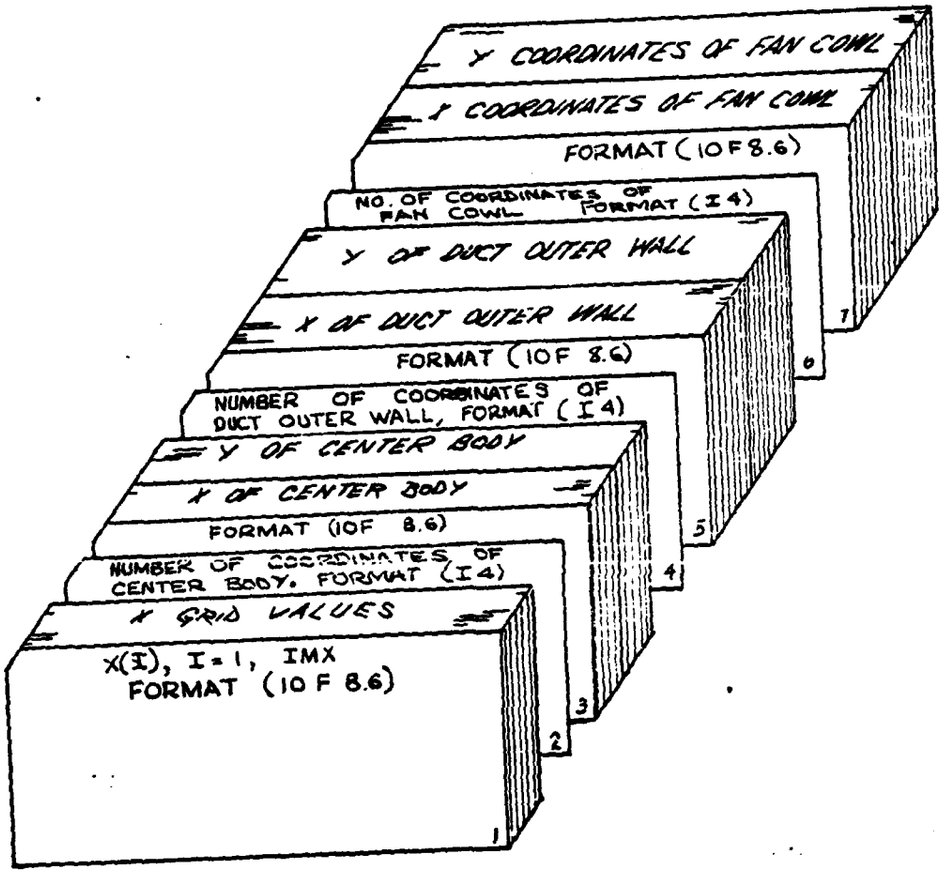

FIGURE 13 SUGGESTED FORM OF INPUT DATA FOR BODY SUBROUTINE WHEN COORDINATES OF CENTERBODY, DUCT OUTER WALL, AND FAN COWL ARE USED TO DESCRIBE THE CONFIGURATION.

2. Subroutine Body

This is the subroutine in which the wall boundary is read and the wall slopes computed at the axial positions of the mesh. The X or axial coordinates of the mesh points are also read in this subroutine with the statement:

```
      READ (5,1010)  (X(I), I = 1,IMX)
1010  FORMAT  (10F8.6)
```

Since the contours for the centerbody, outer walls of the duct, and the fan cowl are not defined in any standard convenient coordinate system, this subroutine at least in part may need to be reprogrammed for each new geometry. The contours are fitted by a spline program, then the values of the radial coordinates and the slopes at the mesh points X(I) are computed. When coordinates are used to describe the contours, the set up of the deck described in Figure 13 is suggested with appropriate read statements included in the BODY subroutine.

The subroutine SPLINE used by BODY to fit the coordinates is called by the statement

```
CALL SPLINE (MODE,N,X,Y,D,E,W,JJ,XB,YB,YP,YPP)
```

Mode should be set to zero at first entry to set up the coefficients for fitting the N points (X,Y) and greater than zero thereafter for finding points on the same curve. XB is the value of the abscissa X at which the value of the ordinate YB is desired. Since the slope boundary conditions are required for the main program, XB are the values of the x grid points X(I) for which the contours are defined. YP and YPP are the first and second derivatives of the fitted curve at the point X = XB. E and W are storage required by t he program and both must be at least 3N

long. The indices JJ indicate whether end points of the fitted curve satisfy the slope or curvature conditions.

JJ(1) = 0 2nd derivative at left end point given by D(1).

JJ(1) = 1 1st derivative at left end point given by D(1).

JJ(2) = 0 2nd derivative at right end point given by D(2).

JJ(2) = 1 1st derivative at right end point given by D(2).

A thickness ratio DELTA and mean dimensionless radii RINNER for the centerbody and RF for fan cowl must be computed in the program from the contour data. RINNER is defined as the average of the smallest and largest radii along the centerbody and is the radius at which the linearized boundary conditions are satisfied. The radial grid is constructed so that RINNER = R(1)-(R(2)-R(1))/2. The thickness ratio DELTA is the difference between maximum and minimum radii of the centerbody divided by its length. For the computed examples, this length was conveniently chosen as the distance from the duct fan plane in Figure 2b to the point of maximum body radius.

Similarly, the mean radius RF at which the linearized boundary conditions on the fan cowl, on the outer duct wall, and on the free jet boundary are satisfied is the average between minimum duct radius and maximum cowl radius. The radial grid is set up so that the midpoint between R(JM) and R(JM+1) is the radius RF. With RF and RINNER computed in the subroutine BODY, the main program computes the radial grid points. Evenly spaced points are computed for the duct flow and the increments between radial positions of the exterior flow are stretched by the factor DRFAC defined in the namelist PARAM.

For the boundary conditions required in the main program, the BODY subroutine must compute the derivatives divided by the value of DELTA for the centerbody, outer duct wall, and the fan cowl. The notation used by the main program is:

RX(I), I = 1 to IMX. Slope of centerbody divided by DELTA.

RLX(I), I = 1 to IO. Slope of outer wall divided by DELTA.

RUX(I), I = 1 to IO. Slope of fan cowl divided by DELTA.

In summary, the subroutine BODY must be programmed to compute RINNER, the mean radius of the centerbody; RF, the mean location of outer duct wall, fan cowl, and free jet streamline boundary; and the slope boundary data RX, RLX, and RUX defined above at the x grid points. The subroutine must also compute the dimensionless radii of the centerbody, RS1; outer duct wall, RS2; and fan cow, RS3, which are required for the subroutine STRMLN.

3. Subroutine STRMLN

This subroutine computes the radial position of the streamlines at the x mesh positions. Along each radial mesh line R(J) the streamline is defined by

$$R_1(X_i) - (R_1(x_1) = \int_{X_1}^{X_i} \left(\Phi_{r_1} / \Phi_x\right) dx$$

where Φ is the complete velocity potential. In terms of the perturbation potential, φ , this becomes, since $r = \tau r_1$ and $\tau\epsilon = \delta$.

$$R_1(x_i) - R_1(x_1) = \frac{\delta M_\infty^2}{M_j^2} \int_{x_1}^{x_i} \varphi_r \, dx$$

for points inside the duct and

$$R_1(x_i) - R_1(x) = \delta \int_{x_1}^{x_1'} \varphi_r \, dx$$

for points outside the duct flow. The derivative φ_r at the points R(J) is found by fitting a polynomial through three adjacent points along a line x constant and differentiating it to find φ_r . The x integration is performed by the trapezoidal rule.

4. Description of Printout

After the printing of the parameter list, the coordinates and slope of the lower and upper fan contours and of the nacelle are printed for values of x corresponding to the mesh points. The actual slopes are printed in the column labeled DER (for derivative). The slopes divided by the thickness parameter are used as boundary conditions in the main program and are designated by RX, RLX, and RUX for the lower fan contour, upper fan contour, and nacelle, respectively. The following is a glossary of the notation used in the printout.

P(I,J) Value of perturbation velocity potential at X = X(I), R = R(J) of the mesh

PHSX Value of φ_x at R(JM).

PHX(I,J) Value of φ_x at X(I), R(J).

R Dimensionless radial variable. (Multiplied by $\tau = M_\infty^{2/3}\delta^{1/3}$ for printout of PHIX).

PHIX Boundary values of φ_x at x = 0.

At every NP iteration through the mesh a partial printout is made for the purpose of monitoring the convergence. At this time, the number of iterations required for each column is printed by two rows of integers in groups of ten. The first row of integers corresponds to the column iteration in the duct for $I \leq IO$ and the entire column for $I > IO$. The second row corresponds to column iterating for the region above the nacelle. The maximum error is printed out next along with the I,J point of the mesh at which it occurs.

At the twelve axial positions designed at ILINE(K) two rows of φ at J=1 and JM are then printed followed by two rows of φ_X at J = JM and 1. The eighth row gives the single quantity $\Delta\varphi$ at X = X(IO), the nacelle trailing edge. Every NA times the value of φ_X at the duct input is calculated, printed, and updated.

In the final printout from the subroutine PRTOUT, the column variables are

CPB	Coefficient of pressure on the body based on the exterior stream conditions.
CPS	Coefficient of pressure on the free streamline based on the exterior stream.
PHI	Value of φ along radial position J = JM.
R-RF	Deviation of free streamline from the trailing edge radial position.

5. Operation of the Program

By means of the intermediate printout every NP times, the rate of convergence of the solution can be monitored. Completely subsonic flows with an initially prescribed uniform flow ($\varphi \equiv 0$, MODIN=1) usually converge successfully. When the jet Mach number is chosen greater than unity, starting with $\varphi \equiv 0$ leads to an immediate arithmetic error stop when the program encounters a negative index for the P(I,J) variables. To find a solution for a supersonic free jet, the Mach number M_j (XMJ) must be increased by small increments such as $\Delta M = 0.05$ or 0.1, starting with a subsonic value and obtaining partial convergence at each Mach number. If the change in Mach number is too great, the solution may take longer to converge or it may diverge. Considerable computing time in obtaining a new solution can be saved by using the P(I,J) grid data from a solution for which the boundaries are similar to the new configuration and the Mach numbers are close to those for the desired solution. Solutions with large imbedded supersonic regions usually make poor starting solutions since they often cause the iterations to diverge.

There are three programmed stops. STOPS 1 and 2 occur with successful completion of the computations. STOP 1 occurs for MODOUT=1 for which no data is punched. STOP 2 occurs for MODOUT=2 for which the potential field is punched on cards as a starting solution for a later run. STOP 3 occurs when the maximum value of the difference between consecutive values of φ exceeds 5, indicating that the solution is diverging.

A quantity important to the convergence is the value of φ_x at the fan plane (PXIN in PARAM list). When only a fair estimate is provided

and the value is not corrected in the iteration process, it was found that the solution converged to a minimum value for the error (ERR) which was greater than 0.0001 and then started to diverge. Improving the value of PXIN caused the solution to converge to a smaller minimum value of ERR before again starting to diverge. In the program, PXIN is updated every NA times by estimating the diameter of the jet far downstream, computing the mass flow rate through this cross section, and determining φ_x (PXIN) which yields this value of the mass flow rate at the fan plane. The value of φ_x determined this way is close to that value of φ_x which leads to the most converged solution but not necessarily equal to it, because of the approximate way of computing the downstream duct mass flow.

References

1. Murman, E. M., "Computational Methods for Inviscid Transonic Flows with Imbedded Shock Waves", Boeing Scientific Research Laboratories Document D1-82-1053 (1971); also as invited lecture series for AGARD-VKI Lecture Series on Numerical Methods in Fluid Dynamics, Rhode-Saint-Genese, Belgium, March 1971.

2. Murman, E. M. and Cole, J. D., "Calculation of Plane Steady Transonic Flows", AIAA J., Vol. 9, No. 1, January 1971, pp. 114-121.

3. Murman, E. M. and Krupp, J. A., "Solution of the Transonic Potential Equation Using a Mixed Finite Difference System", presented at 2nd International Symposium on Numerical Methods in Fluid Dynamics, September 1970; Proceedings published in Lecture Notes in Physics, Springer-Verlag (1971).

4. Krupp, J. A., "The Numerical Calculation of Plane Steady Transonic Flows Past Thin Lifting Airfoils", Boeing Scientific Research Laboratories Document D180-12958-1, June 1971.

5. Krupp, J. A. and Murman, E. M., "Computation of Transonic Flows Past Lifting Airfoils and Slender Bodies", AIAA J., Vol. 10, July 1972, pp. 880-887.

6. Murman, E. M. and Ehlers, F. E., "Proposal for Computing the Transonic Flow Over Nacelles and through Cascades", Technical Communication 63, Aerodynamics and Marine Sciences Laboratory, Boeing Scientific Research Laboratories, June 1971.

7. Krupp, J. A., "Documentation for Program TSONIC", Technical Communication 064, Aerodynamic and Marine Sciences Laboratory, Boeing Scientific Research Laboratories, June 1971.

8. Krupp, J. A. and Murman, E. M., "The Numerical Calculation of Steady Transonic Flows Past Thin Lifting Airfoils and Slender Bodies", AIAA Paper No. 71-566, June 1971 (also included as part of Ref. (9)).

9. Murman, E. M., "Documentation of Program TSONAX", Technical Communication 067, Transportation Systems Research Laboratory, Boeing Scientific Research Laboratories, Aug. 1971.

10. Milne-Thomson, L. M., "Theoretical Hydrodynamics", Fifth Edition, The MacMillian Company, New York, 1968.

END

DATE
FILMED

8-83

DTIC